COMPREHENSIVE CHARACTERIZATION AND ANALYSIS OF ECO-FRIENDLY INGREDIENTS IN TISSUE-EQUIVALENT PHANTOM DEVELOPMENT FOR BIOMEDICAL MICROWAVE APPLICATION

AZIMAH BINTI AZMI

UNIVERSITI TEKNIKAL MALAYSIA MELAKA

COMPREHENSIVE CHARACTERIZATION AND ANALYSIS OF ECO-FRIENDLY INGREDIENTS IN TISSUE-EQUIVALENT PHANTOM DEVELOPMENT FOR BIOMEDICAL MICROWAVE APPLICATION

AZIMAH BINTI AZMI

This report is submitted in partial fulfilment of the requirements for the degree of Bachelor of Electronic Engineering with Honours

Faculty of Electronics and Computer Technology and Engineering
Universiti Teknikal Malaysia Melaka

2024

UNIVERSITI TEKNIKAL MALAYSIA MELAKA
FAKULTI TEKNOLOGI DAN KEJUTERAAN ELEKTRONIK DAN KOMPUTER

BORANG PENGESAHAN STATUS LAPORAN
PROJEK SARJANA MUDA II

Tajuk Projek : Comprehensive Characterization and Analysis of Eco-Friendly Ingredients in Tissue-Equivalent Phantom Development for Biomedical Microwave Application

Sesi Pengajian : 2023/2024

Saya AZIMAH BINTI AZMI mengaku membenarkan laporan Projek Sarjana Muda ini disimpan di Perpustakaan dengan syarat-syarat kegunaan seperti berikut:

1. Laporan adalah hakmilik Universiti Teknikal Malaysia Melaka.
2. Perpustakaan dibenarkan membuat salinan untuk tujuan pengajian sahaja.
3. Perpustakaan dibenarkan membuat salinan laporan ini sebagai bahan pertukaran antara institusi pengajian tinggi.
4. Sila tandakan (✓):

☐ **SULIT*** (Mengandungi maklumat yang berdarjah keselamatan atau kepentingan Malaysia seperti yang termaktub di dalam AKTA RAHSIA RASMI 1972)

☐ **TERHAD*** (Mengandungi maklumat terhad yang telah ditentukan oleh organisasi/badan di mana penyelidikan dijalankan.

☑ **TIDAK TERHAD**

Disahkan oleh:

_____
(TANDATANGAN PENULIS)

_____
(COP DAN TANDATANGAN PENYELIA)
TS. DR. NOOR BADARIAH BINTI ASAN
Pensyarah Kanan
Fakulti Teknologi dan Kejuruteraan Elektronik dan Komputer
Universiti Teknikal Malaysia Melaka
Hang Tuah Jaya, 76100 Durian Tunggal, Melaka
email: noorbadariah@utem.edu.my

Alamat Tetap: GI 352, Lorong siantan 7, kampung seri gombak indah,68100, Batu caves, Selangor

Tarikh : 24 JANUARI 2024   Tarikh : 24 JANUARI 2024

*CATATAN: Jika laporan ini SULIT atau TERHAD, sila lampirkan surat daripada pihak berkuasa/organisasi berkenaan dengan menyatakan sekali tempoh laporan ini perlu dikelaskan sebagai SULIT atau TERHAD.

DECLARATION

I declare that this report entitled "COMPREHENSIVE CHARACTERIZATION AND ANALYSIS OF ECO-FRIENDLY INGREDIENTS IN TISSUE-EQUIVALENT PHANTOM DEVELOPMENT FOR BIOMEDICAL MICROWAVE APPLICATION" is the result of my own work except for quotes as cited in the references.
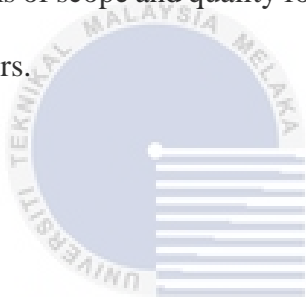
Signature   :   …………………………………

Author   :   AZIMAH BINTI AZMI

Date   :   24 JANUARY 2024
                     …………………………………

APPROVAL

I hereby declare that I have read this thesis and in my opinion this thesis is sufficient in terms of scope and quality for the award of Bachelor of Electronic Engineering with Honours.

Signature : ....

Supervisor Name : Ts. DR. NOOR BADARIAH BINTI ASAN

Date : 24 JANUARY 2024
....

DEDICATION

To my younger self, who decided to choose this path. You did well…

ABSTRACT

The use of animals in research has been a topic of debate due to ethical concerns and the potential harm caused to animals. To address this issue, researchers have been exploring using tissue-equivalent phantoms as an alternative to animal testing. These phantoms are designed to mimic human tissues' physical and chemical properties, making them ideal for testing the safety and efficacy of medical devices and new drugs. This research uses boiling and direct heating methods to characterize and analyze eco-friendly ingredients in tissue equivalent phantom development for biomedical microwave applications. Phantom development methods comprise skin, fat and muscle as semi-solid, flexible, and malleable in the 1GHz to 20GHz frequency range. The dielectric properties of the formed tissue phantom were measured using the performance probe in the Agilent Technologies 85070E dielectric probe kit, and the results were recorded by Agilent Technologies N5242A Vector Network Analyzer (VNA). From the result obtained, each tissue phantom created showed the trend where it could mimic the dielectric properties in relative permittivity and loss tangent compared to the human tissues. This research has offered one of the opportunities in education and medicine since it will benefit the biomedical engineering field and have a long-term impact on the environment and society.

ABSTRAK

Penggunaan haiwan dalam penyelidikan telah menjadi topik perdebatan kerana kebimbangan etika dan potensi bahaya yang disebabkan oleh haiwan. Untuk menangani isu ini, penyelidik telah meneroka menggunakan tisu palsu yang setara dengan tisu mnusia sebagai alternatif kepada ujian ke atas haiwan. Tisu palsu ini direka bentuk untuk meniru sifat fizikal dan kimia tisu manusia, menjadikannya ideal untuk menguji keselamatan dan keberkesanan peranti perubatan dan ubat baharu. Penyelidikan ini menggunakan kaedah mendidih dan pemanasan terus untuk mencirikan dan menganalisis bahan mesra alam dalam pembangunan tisu palsu yang setara dengan tisu sebenar untuk aplikasi gelombang mikro bioperubatan. Kaedah pembangunan tisu palsu terdiri daripada kulit, lemak dan otot sebagai separa pepejal, fleksibel dan boleh ditempa dalam julat frekuensi 1GHz hingga 20GHz. Sifat dielektrik tisu palsu yang terbentuk diukur menggunakan "probe" prestasi dalam kit dielektrik Agilent Technologies 85070E, dan hasilnya direkodkan oleh Agilent Technologies N5242A Vector Network Analyzer (VNA). Daripada hasil yang diperoleh, setiap tisu yang dicipta menunjukkan trend di mana ia boleh meniru sifat dielektrik dalam kebolehtelapan relatif dan kehilangan tangent berbanding dengan tisu manusia. Penyelidikan ini telah menawarkan salah satu peluang dalam pendidikan dan

perubatan kerana ia akan memberi manfaat kepada bidang kejuruteraan bioperubatan dan memberi kesan jangka panjang kepada alam sekitar dan masyarakat.

ACKNOWLEDGEMENTS

I would like to convey my heartfelt gratitude to Allah SWT for blessing me with the ability to complete my thesis writing. I am also grateful to my mother, father, and siblings for their unwavering encouragement, support, and love. I would also like to thank my supervisor, Ts. Dr. Noor Badariah Asan, for her significant guidance, constructive input, and patience during the research and thesis writing process. This thesis would not have been possible without her help. I'd also like to thank my friends whom I've shared my worries with and whoever I have crossed my path on this journey, for inspiration, motivation, and support. Their constant support and friendship have been a source of strength and inspiration throughout my academic career. Last but not least, I would like to thank myself for not giving up and keeping up my momentum to complete this research however hard it was.

TABLE OF CONTENTS

LIST OF FIGURES

LIST OF TABLES

LIST OF SYMBOLS AND ABBREVIATIONS

A	:	Ampere
ECO S1-S5	:	Eco friendly based skin phantom 1-5
ECO F1-F4	:	Eco friendly based fat phantom 1-4
ECO M1-M5	:	Eco friendly based muscle 1-5
CIRS	:	Computerized imaging reference system
CT	:	Computerized Tomography
DI	:	Distilled water
F	:	Farad
SAR	:	Specific Absorption Rate
SRR	:	Split Ring Resonator
SS	:	Semi Solid
S21	:	Scattering parameter
MR	:	Magnetic Resonance

MAS	:	Standalone Microwave Resonator
MUT	:	Material Under Testing
MRI	:	Magnetic Resonance Imaging
PET	:	Positron Emission Tomography
PVP	:	Polyvinylpyrrolidone
PEP	:	Polyethylene Plastics
PPE	:	Personal Protective Equipment
PDV	:	Pure Dried Vacuum
OCT	:	Optical Coherence Tomography
NaCl	:	Natural Chloride
HF	:	High Frequency
GHz	:	Gigahertz
MHz	:	Megahertz
Kg	:	Kilogram
3D	:	3 Dimensional
$tan\ \delta$	:	The loss tangent of dielectric material
ε'_r	:	The real part of relative permittivity
ε''_r	:	The imaginary part of relative permittivity

LIST OF APPENDICES

Appendix A: Spec-Guar Gum

Appendix B: Spec-Maltodextrin

Appendix C: Spec-Sodium benzoate

Appendix D: Spec-Xanthan gum

Appendix E: Spec-Carrageenan gum

Appendix F: Spec-Glycerine

Appendix G: Spec-Sodium alginate
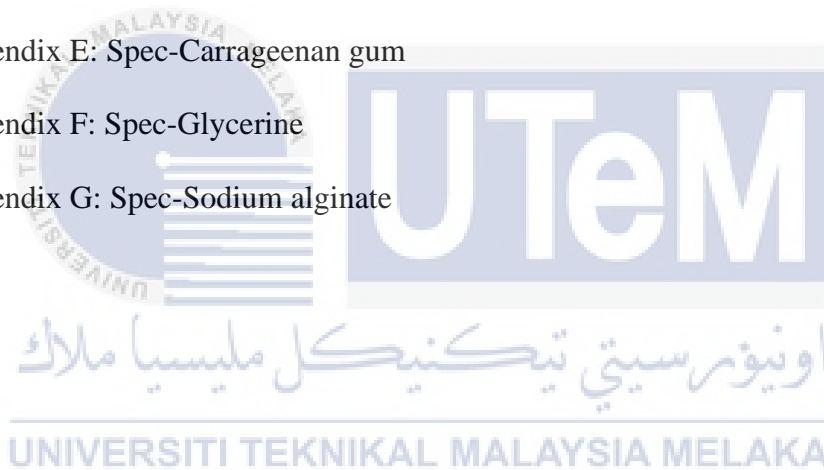
CHAPTER 1

INTRODUCTION

1.1   Overview

This thesis begins a thorough investigation into tissue comparable phantom development for biological microwave applications. This project aims to characterize, analyse, and use sustainable materials in the creation of tissue-equivalent phantoms, with a focus on using eco-friendly ingredients. Tissue-equivalent phantoms are used in medicine to research, validate, manufacture, and evaluate a variety of biomedical devices. The construction of an accurate artificial phantom with three major characteristics: lifelike architecture, precise dielectric properties, and long shelf life is required to mimic human tissue with an exact equivalent [1].

Tissue-equivalent phantoms are in high demand in diagnostic imaging modalities as ultrasonography, MRI, and computed tomography (CT). Other phantoms exist, but the three most frequent are liquid, semi-solid (SS), and solid (dry). The goal of the project is to construct semi-solid skin, fat, and muscle phantoms for biological purposes. The major goal is to gain a thorough understanding of these constituents' properties, their effectiveness in imitating human tissue qualities, and their applicability for high-frequency applications ranging from 1 GHz to 20 GHz. The study is to critically evaluate the identified elements in terms of cost-effectiveness and phantom development durability. This includes determining the long-term durability, practicality, and economic viability of these materials in the creation of tissue-equivalent phantoms appropriate for repeated use and study. The dielectric properties of different tissues in the human body, such as permittivity and loss tangent are vires depending on their kinds and differs significantly depending on the operating frequency [2].

1.2   Problem statement

Every year, there is a significant increase in the use of animal testing for evaluating implanted medical devices and measurements. Preliminary animal tests come before human-centric trials, and they are an important step in the iterative design process. Animal experiments that are successful and meet medical requirements lay the way for later human studies. The imperative, however, is to build a repertoire of eco-friendly elements optimized for tissue-equivalent phantoms, which will serve as a critical paradigm shift. The primary goal is not to eliminate animal testing, but to reduce its frequency.

Efforts are being made to create phantoms that closely resemble human tissues, such as fatty, muscle, and dermal layers. These phantoms can be useful in conducting preclinical evaluations, reducing the need for animal models in clinical trials. This strategic shift attempts to tangibly reduce the reliance on animal testing in scientific settings.

Clinical trials are the principal means by which researchers assess the viability of experimental therapies or preventive measures ranging from medications to dietary interventions or novel medical devices. Adherence to these guiding principles allows the ethical and secure conduct of clinical trials, promoting the development of effective therapies across a wide range of medical settings.

1.3   Objective

- To characterize the eco-friendly ingredients for tissues of equivalent phantom
- To develop the tissue-equivalent phantom in the range 1GHz-20GHz
- To analyse the ingredients for the tissue equivalent phantom development that are cost effective and durable.

1.4   Scope of work
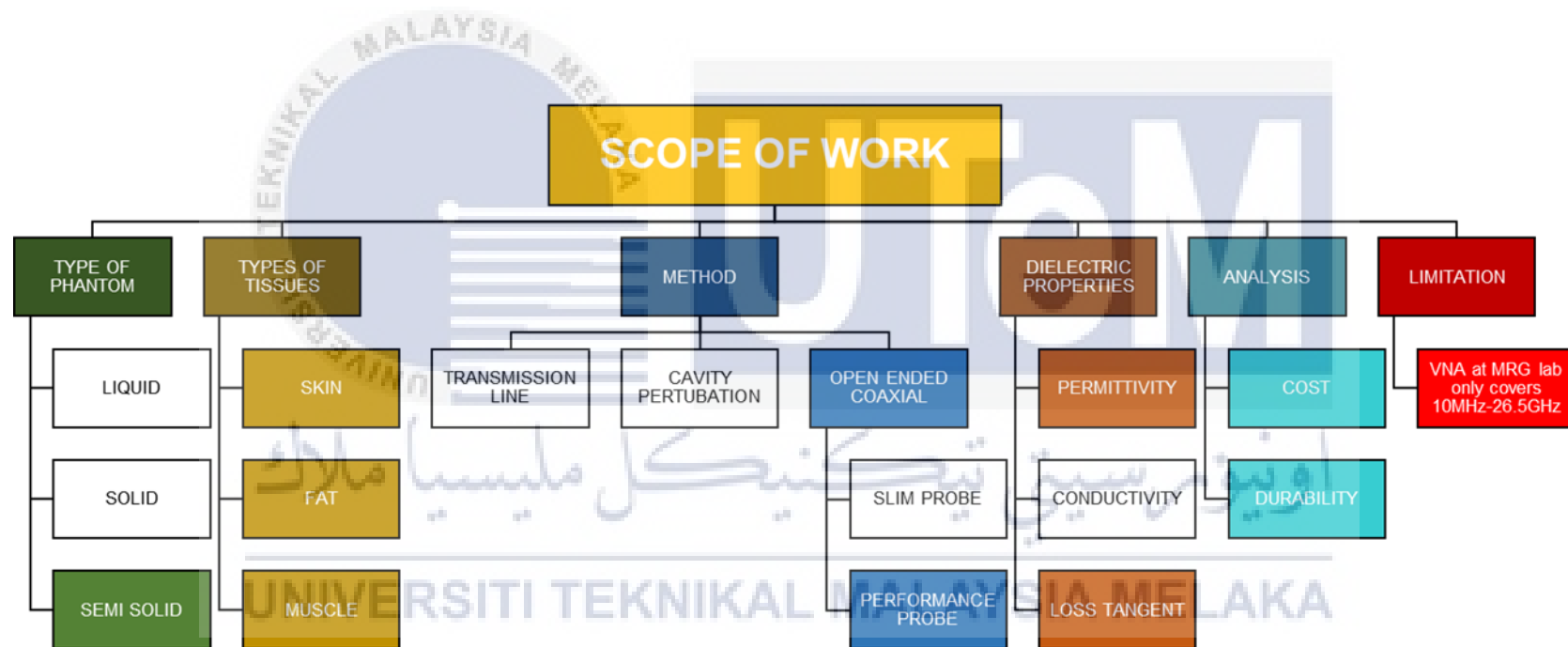
Figure 1.1: Tissue equivalent phantom development scope of work

Previous researchers have laid the groundwork for developing three distinct types of phantoms, namely solid, liquid, and semi-solid, each designed to simulate particular human tissue properties. For this project, the specific focus will be on semi-solid phantoms due to their close resemblance to the structural composition of human tissue, encompassing skin, fat, and muscle characteristics [3].

Numerous methodologies exist in biomedical applications for gauging developmental progress, such as transmission lines, cavity perturbation, and open-ended coaxial methods [4]. In the context of this project, the choice will be to employ the open-ended coaxial and use the performance probe method, primarily owing to its accessibility within the UTEM MRG (Microwave Research Group) lab.

Additionally, the investigation will involve utilizing the performance probe as part of the experimental procedures. The primary objective will encompass the comprehensive measurement of relevant dielectric properties, specifically relative permittivity, and loss tangent [5]. While the assessment of these properties has a history within the field, the emphasis of this study will pivot towards evaluating the cost-effectiveness and durability of phantom development.

However, a notable limitation in this project is the Vector Network Analysis (VNA) operating capacity available in the item MRG lab, which is limited to frequencies up to 26.5GHz. Therefore, the scope of the measurement will be limited from 1GHz to 20GHz only. This poses a constraint as the focus of this study necessitates exploration within the higher-frequency spectrum.

1.5   Thesis structure

The following chapters comprise this thesis: an introduction, a background study, a methodology, a result and discussion, a conclusion, and future work. The project's introduction was explained in Chapter 1. It began with an overview of the background research for the project. All concerns with the ventures were resolved following the context.

The project's purpose is determined by the problem statement, and the scope of work was also considered. The background studies for the project were then discussed in Chapter 2. Based on the project title, a background study was conducted, which included the types of tissue-equivalent phantoms, the dielectric properties of biological tissues, the application of tissue-equivalent phantoms, and the methods used to ensure the phantom's dielectric properties as well as the studies of each ingredient used in tissue phantom development. Background study on the components and materials needed to make tissue-equivalent phantoms was also undertaken.

The flow of the project methodology was provided in Chapter 3. To begin, conduct a review of recent articles and a website focused on project-related topics such as tissue phantom types, the dielectric properties of human tissues (skin, muscle, and fat), the method and recipe for producing tissue phantoms at the desired frequency, and the application used. Moreover, the focus is also on the phantom development using two cooking methods: direct heating and double boiling. Next, based on the information from the literature reviews, the ingredients for the phantom recipe will be finalized and compared to determine the best phantom recipe to replicate the most realistic dielectric properties for each tissue type. After identifying an appropriate phantom recipe, the following step is to fabricate each phantom tissue layer. Finally,

the dielectric properties of the developed tissue phantom will be measured and analysed.

In Chapter 4, the project results were explained, and the results obtained in this proposed project were briefly discussed. The constructed tissue-equivalent phantom's relative permittivity and loss tangent will be addressed. In this chapter the focus does not limit by analysing the comparing tissue phantom between each sample in the term of relative permittivity and loss tangent, but also analysing it within 14 days as the time analysis to ensure the durability of the phantom developed. Furthermore, since some of the ingredients play such a huge impact in the tissue phantom development, the analysis of the ingredients was made to compare each one of it, in the terms of relative permittivity, loss tangent and the texture.

Chapter 5 acts as the dissertation's conclusion, synthesizing the research findings' concluding remarks and providing significant insights and ideas for improving future initiatives to ensure sustainability. This section thoroughly examines the study's findings, emphasizing substantial conclusions and their implications in the context of the research aims. In addition, Chapter 5 attempts to give actionable proposals and strategic improvements that can be applied in the future to increase the efficacy, efficiency, and sustainability of comparable initiatives. This chapter aims to pave the path for more long-lasting and meaningful activities in the relevant field by synthesizing research findings with critical observations and foresight.

CHAPTER 2

BACKGROUND STUDY

The present chapter provides a comprehensive overview of the development of a tissue-equivalent phantom, incorporating findings from previous studies and a thorough literature review. The research process involved comparing various sources of information, including relevant papers, scholarly articles, and websites, to gather and analyse data pertinent to the phantom's development. The following aspects of the phantom were considered and discussed in detail:

- Phantom recipes: The composition of the phantom, including the types of tissues created, were examined, and compared based on their capacity, specifications, attributes, and benefits and drawbacks.

- Frequency range: The range of frequencies used in the phantom was examined and discussed in the context of its application and effectiveness.

- Existing documentation: Relevant literature on various types of tissue phantoms was reviewed to provide a comprehensive understanding of the subject.

The information collected was compared and analysed according to the specifications that are the focus of the research. This comprehensive approach ensured that the resulting phantom met the desired requirements and performed as expected regarding dosimetry and other relevant properties.

2.1 Tissue phantom equivalent development

Tissue-equivalent phantoms are artificial materials that mimic human tissue's mechanical, optical, and electrical properties. Tissue-comparable phantoms are usually used in biomedical engineering for testing, calibrating, and validating various medical devices and drugs. Most of the existing tissue equivalent phantoms are made of synthetic or animal-derived non-eco-friendly, biodegradable, and renewable materials. Therefore, tissue-equivalent phantoms need to be more environmentally sustainable and ethical. Developing tissue equivalent phantoms driven by natural or biodegradable ingredients such as cellulose, starch, and gelatine can achieve different tissue properties by varying the concentration, cross-blinking or blending it [6]. It creates tissue-equivalent phantoms such as skin, muscle, bone, liver, kidney, or heart, including many tissue types or organs. These phantoms can be used to study the relationships and interdependencies between various tissues or organs and the impact of systemic disorders or therapies on the body as a whole. A published study revealed the creation of a multi-organ tissue-equivalent phantom that may be used for

ultrasound-guided needle biopsy or ablation and can replicate the human belly's anatomical and physiological features [7].

2.1.1   Solid phantom

Solid tissue-equivalent phantoms are materials that mimic human tissue's physical and radiological characteristics in various ways, including radiation therapy and medical imaging. These phantoms are made to closely resemble human tissue's absorption and scattering coefficients at particular wavelengths. These phantoms can have a variety of materials inside of them, but to mimic the optical characteristics of natural tissue, materials like titanium dioxide particles, epoxy resin, and near-infrared dye nowadays made of 3D printing modelling are frequently used and costly. Solid phantoms are helpful for dosimetry verification and planning in medical treatments, and they can be created from materials like plastic, polymers, silicone, and wax. Solid phantoms are necessary for reproducing the optical characteristics of human tissue precisely, even though they may be less flexible to make than liquid phantoms [8] [9].

Figure 2.1: A Physical Human Phantom Study [10].

2.1.2   Liquid phantom

Phantoms that are liquid-based tissue equivalents are employed in medical research to replicate the characteristics of human tissue. It is a liquid used to fill a container to create a sealed phantom that meets the requirements for body phantoms. Low yield stress and colloidal stability are two characteristics of the liquid that are intended to be similar to those of soft tissue; the tissue-equivalent nature of the liquid is confirmed by measuring its dielectric properties. The benefit of liquid phantoms is their capacity to bridge gaps in produced phantoms, including intricate geometries [11].

Liquid phantoms are a valuable option for various biomedical applications due to their ease of preparation and management of volume and consistency. Flexibility: liquid phantoms can be quickly controlled and managed to change their attributes. Filling voids: Liquid phantoms can fill voids in produced phantoms, even those with intricate geometries that qualify for various uses [12]. In the terms of dielectric characteristics: Liquid phantoms can have dielectric characteristics that are similar to those of human tissues, allowing them to be used in several medical research applications, including thermal treatment investigations and SAR assessment [13].
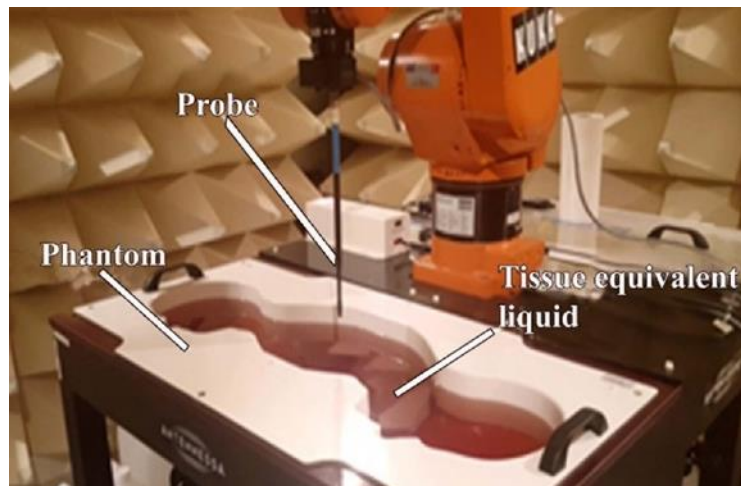
Figure 2.2: Analysing the SAR in Human Head Tissues under Different Exposure Scenarios [14]

2.1.3   Semi-solid phantom

Semi-solid phantoms are tissue mimics in biomedical applications, including microwave imaging and thermal characterization. They imitate human tissues and come in low-cost varieties with a multi-layered heterogeneous structure, substantial shelf life, and mechanical and electrical stability. Hydrogel-based phantoms, such as agarose and gelatine matrices, are semi-solid phantoms. It is made of mostly Agar and gelatine to adjust relative permittivity and construct a semi-solid structure. It was used to estimate strokes in microwave-based imaging systems [15].

Semi-solid phantoms provide advantages such as being easy to produce and bendable and tuneable optical characteristics. It was used to test and evaluate medical equipment and systems in various domains, such as thermal characterization and microwave imaging [16] .
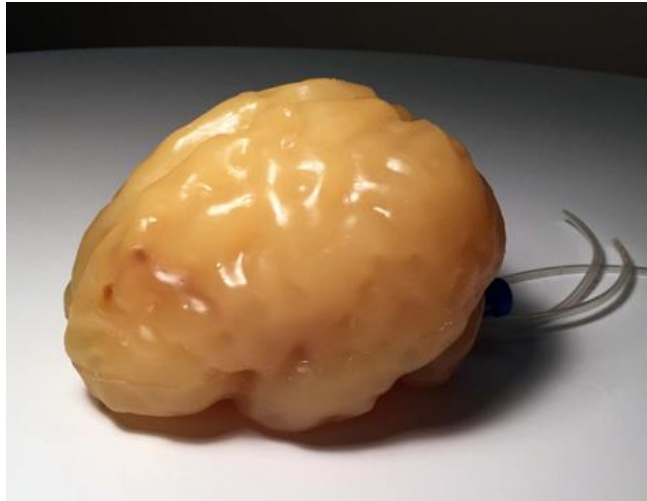
Figure 2.3: Example of semi solid phantom [17]

2.2   Skin Tissue Phantom

The extremely challenging nature of the proposed methods for their development poses a significant obstacle to the manufacturing of phantom tissues. Additionally, the specificity of the variations or the complex, layered structure of biological tissues to be mimicked is limited by the quick deterioration and low temporal durability of commonly utilized phantom materials [17]. Therefore, this research aims for using eco-friendly and affordable substances but durable, to substitute the available tissue phantom that are currently used in the medical industry. For optical imaging research, a single-layer skin comparable tissue phantom with inner vascular channels was created in 2014 [18].

Developing a substance with characteristics like human skin in terms of its physical and chemical composition is necessary to build a tissue-equivalent phantom. This can be done by altering the content of various substances, like water, glycerine, and gelatine, to simulate the characteristics of tissues, such as skin. The result is then put through testing to make sure it precisely replicates the

characteristics of human tissue and may be used as a replacement in medical imaging and medical treatments.
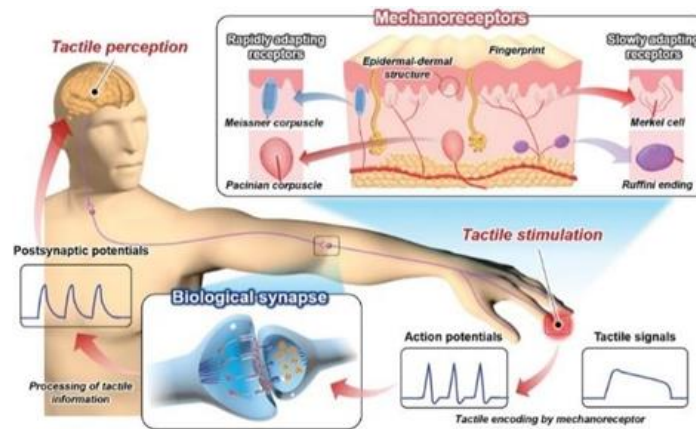
Figure 2.4: Mimicking Human and Biological Skins for Multifunctional Skin Electronic

2.3 Fat Tissue Phantom

A fat tissue equivalent phantom is a material that mimics the properties of human fat tissue and is used in various medical applications. Fat tissue equivalent phantoms allow researchers to test and develop medical technologies without the need for human subjects. Besides, it is can also be used to compare different imaging techniques for the quantification of fat and it can be used to create imaging and therapy phantoms which are widely use in the medical imaging field. Furthermore, it can be used in Raman spectroscopy for biomedical applications [16].

The CIRS BR3D Model 020 phantom, which uses two resin tissue-equivalent materials that simulate 100% glandular and adipose tissue swirled together in a set, is an example of a fat tissue equivalent phantom in real life [19]. This phantom is used to create imaging and therapy phantoms in the medical field to treat the patient with related diseases.

2.4   Muscle Tissue Phantom

In order to imitate the characteristics of human muscle tissue for medical imaging and for medical treatment, muscle tissue equivalent phantoms are used. Materials called muscle tissue equivalent phantoms are employed in medical imaging and treatments because they have characteristics similar to those of real muscle tissue. A multi-layered, tissue-equivalent phantom including layers of muscle, fat, and skin was proposed in the high frequency (HF) band in 2019 [17]. Compared to other types of phantoms, muscle tissue equivalent phantoms can offer a more accurate portrayal of human muscle tissue.

As the tissue equivalent to muscle increases and the awareness of advancing the technology are increases too, the demand in the industry has led to the new development that involves of the most ecofriendly and durable materials to be commercialize in the medical field as well as biomedical engineering field. An analysis of physical phantoms for brachytherapy conducted in 2021 revealed a rise in interest in magnetic resonance (MR) tissue imitating materials, which is not yet reflected in commercial phantoms for brachytherapy [20]. They can be used to train medical personnel and test and improve imaging and treatment techniques and technology.
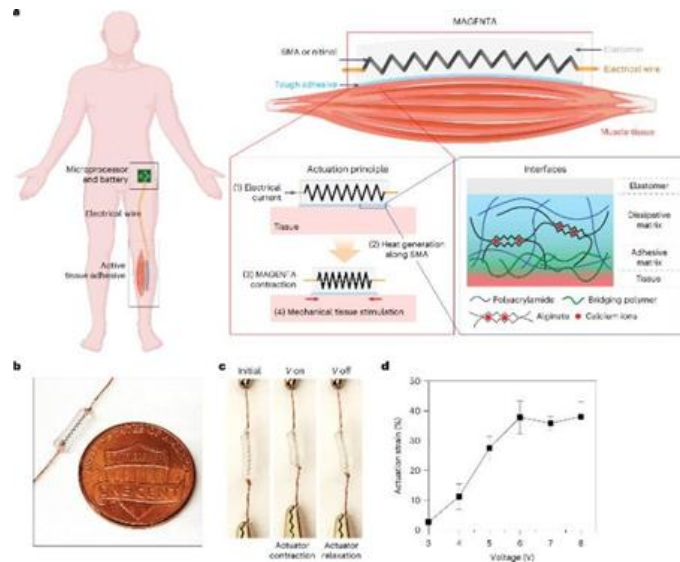
Figure 2.5: Example of muscle phantom application in biomedical engineering field

2.5 State of art on tissue equivalent phantom from previous paper

Table 2.1: State of art tissue equivalent phantom from previous paper

Ref.	Tissue	State of matter	Frequency	Main finding	Objective	Application	Limitation
[21]	Brain	Semi solid	1-10 GHz	The research describes the creation of a tissue-mimicking (TM) phantom with qualities close to human brain tissue for photoablation	To design and adjust the elastic property of a BM phantom, as well as to investigate the response of a tuned BM phantom to photoablation.	tissue mimicking phantom that is suitable for photoablation investigations and subsequent visualisation	The study's limitations include probable discrepancies in computed values compared to earlier work, the shorter shelf life of generated phantoms, more examination of relationships between components, and additional tests and future work.

				investigations and visualisation.			
[22]	Breast	Semi solid	18-40 G Hz	The experimental evidence of penetration depths is in a few centimetres in tissue-mimicking breast phantoms	to develop and test a unique millimetre-wave imaging system for early-stage breast cancer diagnosis and to show the potential use of millimetre-waves to image non-superficial neoplasms in the breast.	early diagnosis of breast cancer has been proposed and tested on several breast phantoms. The system can obtain greater resolution for breasts with high adipose tissue volume and disproves the belief that millimetre-waves are unable to penetrate far enough for	The proximity of the propagating electromagnetic wave, which is a spherical wave due to the near-field region of the antennas, is one of the study's constraints, as is the suggestion for future enhancements incorporating specialised transmit and receive modules and a larger number of physical antennas.

					practical biological applications	
[23]	Human head	Semi solid	1-4 GHz	The dielectric properties of produced brain tissues were found to be near those of actual brain tissues, and experimental imaging results indicated the validity of the suggested six-layered tissue	To create a six-layered heterogeneous tissue-imitating head phantom that mimics genuine head tissues and to step-by-step measure and fill the produced tissues in a 3D commercial human skull model, including benign and	Detecting brain strokes and assessment of the phantom's stroke detection capability.	-

			imitating phantoms for brain tumour diagnostics.	malignant tumour (s), for evaluating imaging performances.		
[24]	Human torso- (fat, muscle & blood)	Semi solid and liquid	300K Hz-40M Hz	EIS has the potential to estimate blood flow-induced artery variation. Multiple frequency measurements may increase the accuracy of SF-BIA for hemodynamic monitoring, and EIS	to evaluate the viability of using multi-frequency bioimpedance analysis for hemodynamic assessment, as well as to investigate the use of electrical impedance	Provides an affordable, repeatable, and reliable method for studying tissue dielectric response	The study's limitations include the need for EIS improvements, the need for a more extensive clinical investigation, an emphasis on improving the estimation of constants k and c, a lack of research on impedance phase changes, consideration for frequency selection or weighted

			has the potential to improve current hemodynamic monitoring systems.	spectroscopy (EIS) for assessing changes in radial artery diameter caused by blood flow		frequency contribution criteria, and a lack of research on impedance phase variations.
[25]	Fat	100 M Hz-1 G Hz	Solid and semi solid	Dielectric characteristics of the nanocellulose-gelatine and stabilized emulsions examined. The conformity of the emulsions with	To develop tissue-mimicking phantoms for microwave diagnostics and treatment, to investigate the potential of cellulose nanocrystals reinforced gelatine	Assessment conducted for quality control standards in superficial hyperthermia.	Not fully satisfying the thermal equivalency required for hyperthermia, a lack of examination of the behaviour of the CNC-gelatine reinforced phantom at more excellent heating rates, and the need for additional studies on the

			quality control standards assessed.	emulsions for mimicking fat tissue, and to demonstrate their suitability as fat phantoms for microwave diagnostics and treatment.		phantom's response to protracted stress.
[26]	Blood and Muscle	20 Hz-1 M Hz	Semi solid and liquid	the successful classification of diverse tissue types utilising the designed needle-based electrical	To design a needle-based electrical impedance imaging system, demonstrate its practicality as an alternative, and	Consistency observed in conductivities of the phantoms. Reliability of impedance-based venous entrance	-

				impedance imaging technology, with a focus on fat tissue phantoms' high success rate	assess the performance of the needle navigation system through future hardware and algorithm enhancements, as well as usability testing.	tests demonstrated on layered tissue	
[27]	Breast	0.5-50 G Hz	Semi solid	Demonstrates the ability of the specified recipes to replicate breast tissues with varying	To propose a method for creating, characterizing, and conserving realistic breast tissue-	Creating heterogeneous breast phantoms for mm-wave imaging	The toxicity of commonly used ingredients, the requirement for complex and expensive fabrication equipment, characterization in a limited

				biological features, and the permittivity of mixes made of sunflower oil, water, and gelatine was tested in the 0.5-50 GHz frequency range.	simulating phantoms for testing mm-wave imaging prototypes and to introduce a technique for creating phantoms capable of mimicking several categories of human breast tissues.		frequency range, and the lack of quantitative recommendations for the rational design of phantoms with required electromagnetic properties are all factors.
[28]	Rectus Femoris (muscle)	4-13 M Hz	Semi solid	Various factors, such as thickness, cross-sectional area, and echogenicity, were discovered to	To study the effect of different situations on ultrasound measurements and evaluate the	developed a novel phantom model for rectus femoris muscle ultrasound measurements, which was utilized to test	The phantom model not completely reflecting human subjects, limited information about the phantom model's material, differences in actual

				alter ultrasound measures, and phantom training enhanced measurement accuracy for multiple levels of healthcare workers.	phantom's usage for teaching other health care practitioners.	measurement accuracy and for training purpose	size from the design, a lack of complete standardisation in scanning settings, a limited number of volunteers for the training, and the absence of a comparison between phantom training and traditional ultrasound training without phantom.
[29]	Bone, tissue, muscle, air	none	Liquid, semi solid and solid	The benefit of radiotherapy phantoms in enhancing dosimetry accuracy,	To analyse various forms of phantom materials, investigate the theory of radiotherapy	Use of radiotherapy phantoms to enhance precision in radiation dosimetry measurements.	Inherent uncertainties in treatment planning and execution, the difficulty of adequately mimicking the human body, the insufficiency

				the necessity of quality assurance programs in reducing insufficient treatment and accidents, and the development of anthropomorphic heterogeneous phantoms for particular radiation dosage verification.	phantoms, and highlight the requirement for designing a phantom made of radiation-absorbing materials	Moreover, evaluation of energy absorbed by the human body	of current phantoms to meet dosimetry standards, and the need for low-cost material progress for precise characterization
cavities and teeth							

| [30] | Head and brain | 1 KHz-1 MHz | Solid | The constructed head phantom has great anatomical realism and can represent either a healthy or wounded brain. utilised to create realistic phantoms for electrical impedance tomography examinations of most tissue sets. | To develop dielectrically accurate, easy-to-mould solid (TMMs) for use with electrical impedance tomography and combine it into a realistic head phantom with modifiable pathological lesions. | Creation of a two-layer head and brain phantom And the demonstration of the usefulness and flexibility of tissue imitating material | Uncertainty in dielectric properties due to different internal and extrinsic causes, as well as a band of uncertainty around the reference values for AC conductivity |

2.6   Dielectric Properties

"Dielectric properties" refers to a material's electrical characteristics that influence its behaviour upon exposure to an electric field. These characteristics are linked to the material's electrical energy transmission and storage capacity. A material's dielectric characteristics measure its capacity to transfer charges in response to an external electric field [31]. A dielectric material experiences a polarization effect when an electric field is applied, which causes the electric charges inside the material to move slightly from their equilibrium positions. This polarization develops Positive and negative charges on the material's opposing sides. Several essential factors help define a material's dielectric properties, such as permittivity, conductivity, and loss tangent.

2.6.1   Relative permittivity

Relative permittivity (εr), often known as the dielectric constant, measures a material's capacity to store electrical energy in an electric field. It displays the proportion of the electric field in a substance to that in a vacuum. A substance can store electrical energy more effectively the more significant the dielectric constant. Relative permittivity is dimensionless but can be represented as a number or complex value to account for the material's loss properties. Lossy materials exhibit a fundamental part (εr') and an imaginary part (εr'') of relative permittivity, representing the material's ability to store energy (εr') and the energy dissipated as heat (εr''), respectively.

The capacitance, C, of a condenser with the material between parallel plates of area A and separation d or the force, F, between two charges Q1 and Q2 at a distance r in the material. Both are used to describe a material's permittivity (ε). The relationships,

expressed in SI units as kg–1m–3s4A2 (A = ampere) or F/m (F = farad), exclude any arbitrary numerical factors and are as follows. The dielectric constant, denoted by k, is a quantity that measures the capacity to store electric charges in an applied electric field relative to a vacuum.

$$-k = C/Co$$

where,

c = capacitance of a capacitor with dielectric material.

c_o = capacitance in a vacuum without dielectric material.

The relative complex permittivity ($\varepsilon,\varepsilon_r$) with respect to free space can be defined as:

ε = The permittivity of substance

ε_o = The permittivity of vacuum or free space

The imaginary permittivity can be related to conductivity (σ), and the angular frequency [$\omega = 2\pi f \omega = 2\pi f$] as:

$\varepsilon'' = \sigma/\omega$

$\varepsilon''_r = \sigma/\omega\varepsilon_o$

$$\varepsilon r = \frac{\varepsilon}{\varepsilon O} = \varepsilon' r - \varepsilon''$$

2.6.2 Loss tangent

The tangential component of a material's dielectric loss (tan δ) represents the quantitative loss of electrical energy resulting from various physical processes, including electrical conduction, dielectric relaxation, dielectric resonance, and loss from non-linear processes [32]. A unit of measurement or percentage is frequently used to indicate the dimensionless quantity known as the loss tangent. A higher loss tangent denotes greater energy loss in the dielectric substance. Loss tangent is frequency-dependent, which means that it can change depending on the applied electric field frequency.

Loss tangent is defined as the ratio of the imaginary part of the complex permittivity (ε") to the real part of the complex permittivity (ε'). Mathematically, it is expressed as:

$$\text{Loss tangent (tan } \delta) = \varepsilon'' / \varepsilon'$$

Where, ε" represents the imaginary part of the complex permittivity, which is related to the energy dissipated as heat in the material due to dielectric losses. ε', on the other hand, represents the real part of the complex permittivity, which is related to the energy stored in the material as an electric field.

2.7 Summary of Human Tissue's Dielectric Properties

Table displays the dielectric characteristics of human tissues (skin, fat, and muscle) in the 1–50 GHz frequency range. The Italian National Research Council website [33] is the data source, and published those findings in 1996 [34] [35]. The data was extracted as depicted in Figures to ascertain the relationship between the dielectric characteristics and frequency. Figure 2.8.1 displays the relative permittivity

graph for skin, fat, and muscle in the 1–50 GHz range. The highest relative permittivity is found in muscle, fat, and skin.

On the other hand, the trend indicates that the permittivity decreases with decreasing frequency. The conductivity graph for muscle, fat, and skin in Figure 2.6 displays the conductivity graph for muscle, fat, and skin in the 1–50 GHz range. While fat is inversely proportional to frequency and has the lowest value, skin and muscle are directly proportional to frequency and have nearly comparable values. In the 1GHz–50 GHz range, the skin, fat, and muscle loss tangent trends are directly correlated with frequency, as seen in Figure 2.7

Table 2.2: Summary of Human tissues relative permittivity and loss tangent

Tissue	Relative Permittivity	Loss tangent
Dry Skin	40.9 – 9.4	0.4 – 1.3
Fat	5.4 – 3.2	0.2 – 0.3
Muscle	54.8 – 15.0	0.3 – 1.2
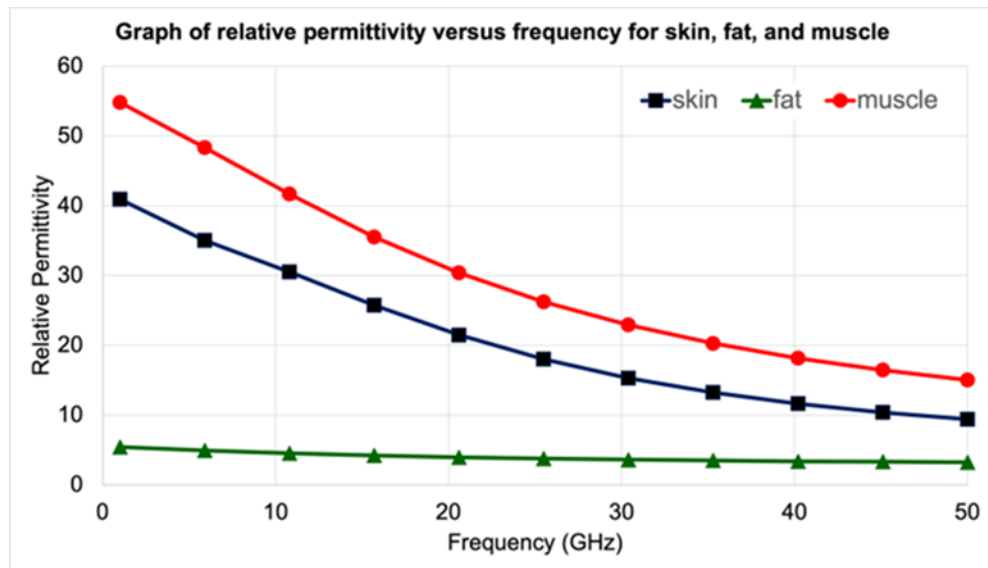
Figure 2.6: The relative permittivity versus frequency (1–50 GHz) for skin, fat, and muscle.
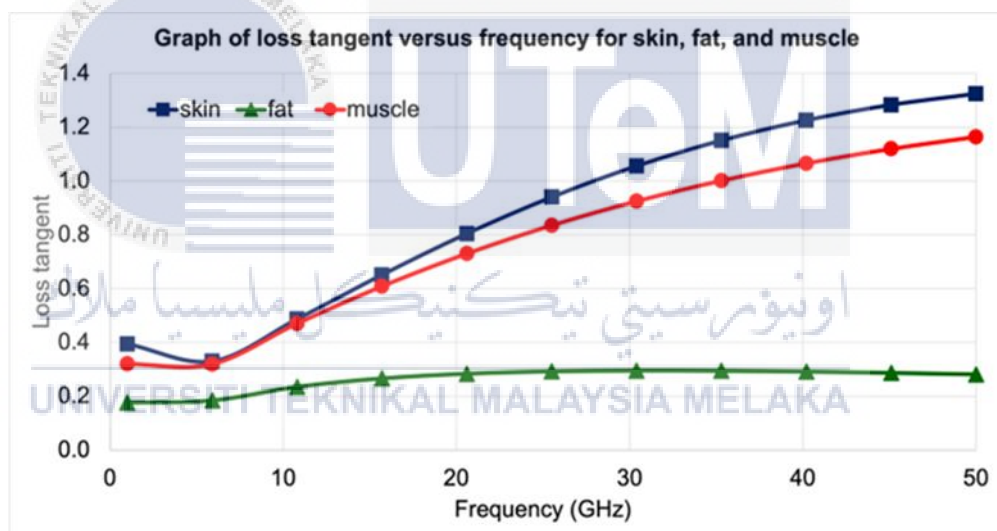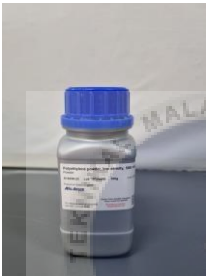
Figure 2.7: The loss tangent versus frequency (1–50 GHz) for skin, fat, and muscle.

2.8   Lists of Ingredients, Characteristics, And Functions

Table 2.3: Ingredients, characteristics, and functions used to develop tissue-equivalent phantom.

Ingredients	Characteristics	Functions
Water	Act as a solvent agent or main ingredient in the solution.	Contributes significantly to the relative permittivity at high frequencies [7].
Distilled water	The purest forms of water available. The distillation process removes most impurities, including minerals, salts, chemicals, and microorganisms. It is essentially free from contaminants.	Ideal for preparing chemical solutions, conducting experiments, calibrating equipment, and cleaning laboratory apparatus. Its purity ensures that impurities do not interfere with the desired properties or stability of the product [36].

Glycerine	Glycerine is highly soluble in water and most organic solvents. It forms clear solutions when mixed with water and can easily dissolve other substances	Glycerine has moisturizing and emollient properties, which means it helps to attract and retain moisture [37].
Polyethylene powder	offers excellent chemical resistance and is resistant to most solvents, alcohols, dilute acids, and alkalis	Can be used as an effective curing agent for TDI and MDI formulations, resulting in improved strength
Propanol	A clear, colourless liquid with a characteristic alcoholic odour	It is useful as a medium- volatility alcohol for improving the drying characteristics of alkyd resins, electrodeposition, paints, and baking finishes

Gelatine	A mixture of peptides and proteins produced by partial hydrolysis of collagen extracted from the skin, bones, and connective tissues of animals	Used as a gelling agent in food, pharmaceuticals, photography, and cosmetic manufacturing. It is used to give food products a jelly-like texture and to stabilize foams and emulsions [38] [39]
PDV Salt	Higher purity than solar salt. It is formed by the artificial evaporation of treated brine in a near vacuum	Sodium chloride (NaCl) can control the conductivity of the phantom [12] [40].
Agar powder	A mixture of two polysaccharides: agarose and agaropectin. Agarose makes up about 70% of the mixture, while agaropectin makes about 30% of it.	It is used to stabilize emulsions and foams also commonly used as a thickener [39] [38]

Hydroxyethyl cellulose	A non-ionic water-soluble polymer made from cellulose, readily soluble in hot and cold water but is insoluble in most organic solvents	Commonly used as a thickener, binder and stabilizer in cosmetic, and pharmaceutical industries.
Sodium Alginate	Soluble in water and forms a viscous solution	As a texturizer, emulsifier, and thickener in the food industry as well as medical applications, including wound dressings and drug delivery systems
Carrageenan Powder	Soluble in water and forms a viscous solution and highly sulphated galectin that is a strongly anionic polymer	As a thickening, gelling, stabilizing, and suspending agent, mostly used for thickener and emulsifier

Maltodextrin	Complex carbohydrate that is produced from starch and readily soluble in water and forms a viscous solution	As a filler and binder in tablets and capsules. It is also used as a carbohydrate supplement for athletes. It is used to provide a quick source of energy during exercise
Sodium Benzoate	The sodium salt of benzoic acid and exists in this form when dissolved in water, almost odourless or exhibits a sweet, faint, balsamic odour and a sweet-sour to acrid taste.	used to prevent the growth of bacteria, yeast, and fungi in various food products, including soft drinks, fruit juices, and pickles.
Guar gum	Soluble in cold water and forms a viscous solution, a hydrocolloid that has thickening and stabilizer	as a thickening, gelling, stabilizing, and suspending agent

Xanthan gum	Soluble in cold and hot water and forms a viscous solution. It is a highly negative charged polymer that enhances hydration	as binder and disintegrant in tablets and capsule, as well as thickening, stabilizing, and emulsifying agent.
Canola oil	A type of vegetable oil that is low in saturated fat and high in monounsaturated and polyunsaturated fats. It is rich in omega-3 fatty acids and has a high smoke point	as a lubricant, free of sediment, is low in saturated fat and high in monounsaturated and polyunsaturated fats [39] [36] [37]
PVP K-90	Can be used as a dispersion to help ensure that particles are distributed uniformly in a liquid medium and can be used to alter the viscosity of liquid formulations, giving them a thickening effect.	may be used in a variety of formulations as a stabilizing ingredient. By preventing the degradation of ingredients, it helps increase the stability and shelf life.

Soy lecithin	Keeps substances like oil and water together that might otherwise separate. It stabilizes mixes so that layers don't form as well as don't separate.	As an emulsifier, soy lecithin keeps substances like oil and water together that might otherwise separate. It stabilizes mixes so that layers don't form as well as don't separate.
Sugar	Biocompatible and non-toxic, allowing them to be used in experiments without endangering researchers or patients' health. This property is very useful for in vitro research and medical imaging calibration.	By controlling the concentration and viscosity of sugar solutions, tissue phantoms can replicate the mechanical properties of certain soft tissues, aiding in the development and calibration [37]

CHAPTER 3

METHODOLOGY

The present chapter provides a comprehensive account of the development of a tissue-equivalent phantom. The chapter offers a concise yet detailed description of the methodology, including selecting materials and ingredients, the fabrication process, and the calibration and measurement procedures. The research journey is also documented, highlighting the challenges and successes encountered during the development of the phantom. Overall, this chapter serves as a valuable resource for researchers and practitioners seeking to develop tissue-equivalent phantoms for various biomedical engineering applications.

3.1 Flowchart of the Project
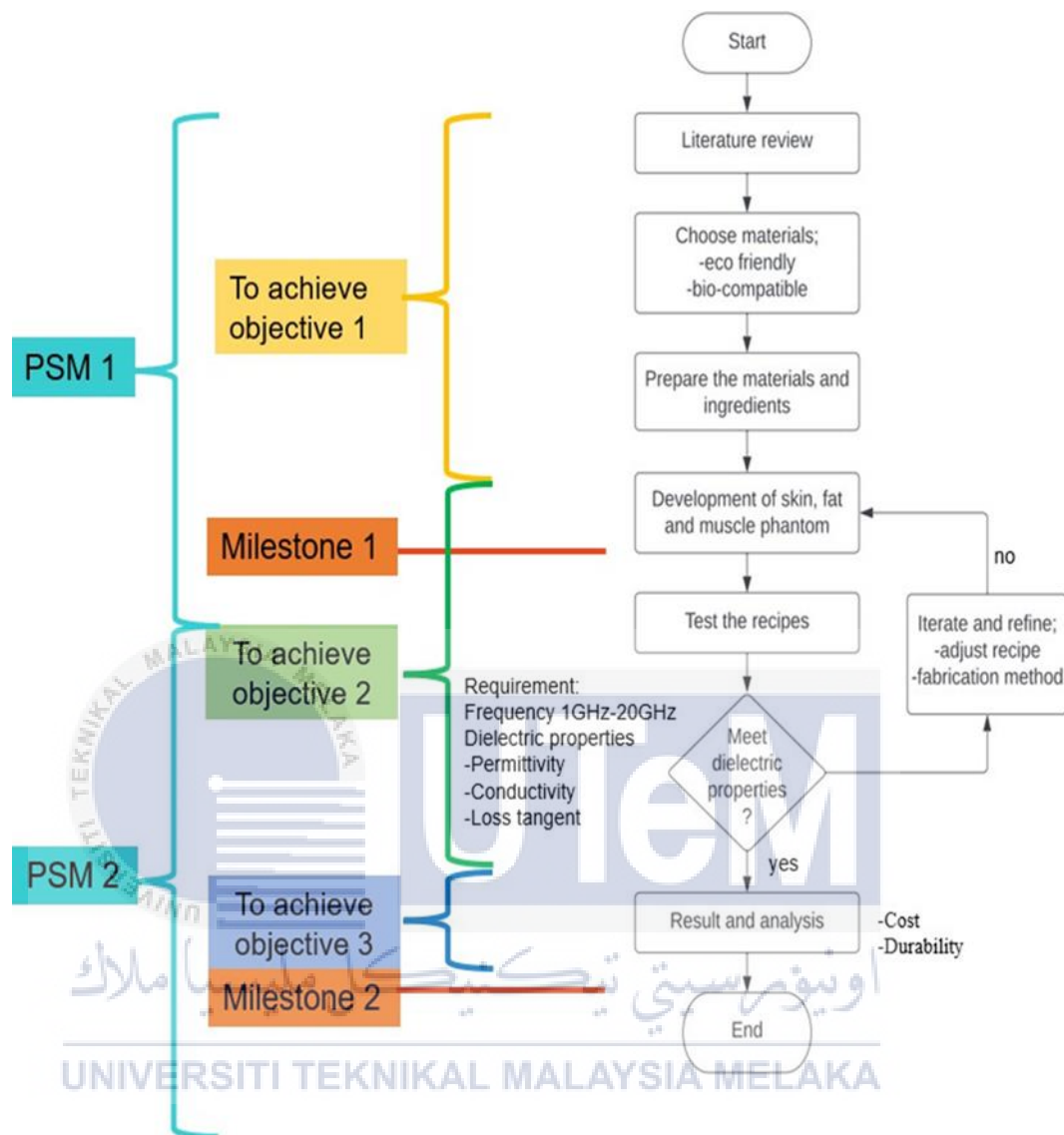
Figure 3.1: Project milestone and flowchart

Mimicking phantom tissue involves a series of steps to create a material that can replicate the properties of human tissue: fat, skin and muscle for various applications such as medical imaging, radiation therapy, and surgical training. The first step is to determine the properties.

The tissue about to mimic, such as density, composition, and mechanical properties, can be done by the literature review for the whole semester during the studies of the phantom mimicking. Next, choose a base material, the starting point for creating the phantom tissue. The most common materials used are water, gelatine, silicone, and other chemical ingredients to replicate the phantom according to the different purposes of the medical needs [42]. Then, the experiment begins with the appropriate equipment used to experiment. The foundation material is modified to match the qualities of the target tissue by adding fillers and additives. If the material is intended to replicate bone, for instance, a filler like hydroxyapatite may be added to increase the density and stiffness of the substance.

During the research, the desired attributes and the developed mixes must be tested. It is appropriately combined and evaluated to ensure the combination has the appropriate qualities. Measuring the material's mechanical, imaging, or other pertinent qualities may be part of the testing process. When the material does not have the intended qualities, the recipe changes, and the process is repeated until the desired properties are obtained. This is known as the refine and iterate process; this process ensures the targeted dielectric properties can be achieved by performing the coaxial probe calibration. Then, the created and replicated phantoms are safely stored in the refrigerator and tested using the desired frequency to ensure their mailability and suitability for tissue engineering applications. Finally, the phantom tissue is tested for data analysis, and accurate results are obtained with the goals of this project to produce new potential or existing ingredients that are bio-compatible and cost-effective to the environment while ensuring its durability for extended-span usage.

3.2 Preparation

The ingredients for the phantom recipe will be finalized and compared based on the knowledge obtained from the literature research to determine the optimal phantom recipe to imitate the most realistic dielectric characteristics for each type of tissue layer.

- Each ingredient's characteristics must be examined during this process to create a tissue phantom that is stable and good for a long time without significantly changing in electrical or physical properties, allowing for multiple tests and measurements for a variety of applications.

- Materials and ingredients are purchased according to the recipe from the literature review.

- The next stage is to create each layer of tissue phantom after choosing the optimum phantom recipe. During this phase, many phantom types will be created simply by changing the proportions of the recipe's ingredients.
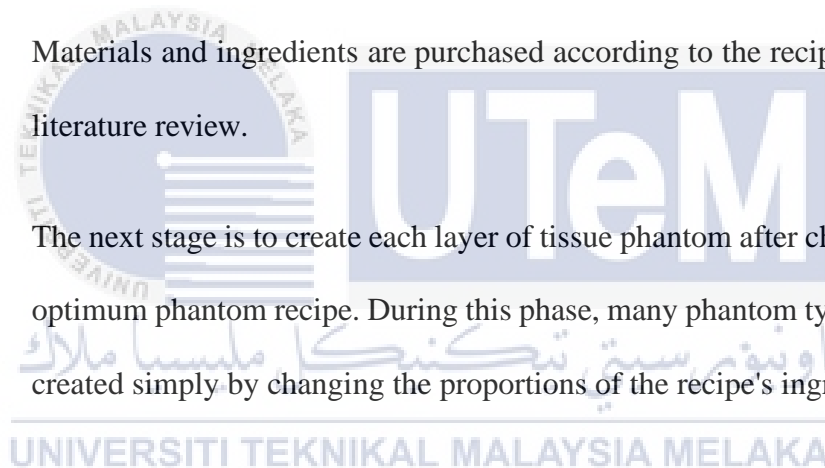
3.3 Development

3.3.1 Development of the tissue equivalent phantom

Based on their biocompatibility, mechanical attributes, and capacity to mirror the characteristics of human tissue, in this analysis, the selection must be catered to choose most suitable biodegradable materials. Then, during the development there will be tried and error out various material ratios and combinations to get the desired characteristics, such as elasticity, tensile strength, and appearance; malleable. Through

iterative testing and analysis, optimize the formulation while considering elements like degradation rate, stability, and cell interaction.

3.3.2 Mechanical and physical characteristics

To compare the performance of the tissue equivalent to that of human muscle and skin, subject it to intensive mechanical and physical testing has been done and supervised by the supervisor. Besides, evaluation of the elements such surface texture, elasticity, tensile strength, and compression resistance must be considered after the phantom development is done.

3.3.3 Eco-friendliness evaluation

Analyse the generated tissue equivalent's lifetime effects on the environment. This development also includes the environmental impact, including resource consumption and waste creation, perform life cycle; how long does the tissues will last be compared with the dielectric properties. In this tissues development also, the comparison between the tissue equivalent's environmental friendliness to that of traditional materials utilized in comparable applications.

3.4 Tissue equivalent-phantom development method

There are two types of method used in the tissue equivalent phantom development which is the double-boiled method and direct heating.

i. Double-boiled method - In constructing tissue-equivalent phantoms, the double boiling approach creates robust and flexible tissue-mimicking materials with realistic qualities that accurately mirror human tissues. This method immerses a container containing the components in an

outside pot of boiling water, providing for moderate and constant cooking while avoiding water evaporation and direct heating [41].

ii. Direct heating method- Involves immersing a substance in a hot environment, and heat transfer happens due to the temperature difference between the material and its surroundings [42]. The creation of tissue-equivalent phantoms for direct heating techniques necessitates careful consideration of the materials and methods used to guarantee that the phantoms accurately duplicate the properties of biological tissues and allow for precise evaluation of heating patterns and effects [43].

For all the tissue-equivalent phantom, both methods have been tried to develop all the tissues to study which method can produce the most suitable relative permittivity and loss tangent according to the iFac reference studied according to the frequency range measured (1GHz-20GHz); from the observations the Skin and Muscle has the high relative permittivity value, therefore the direct heating method has been choose to achieve the high permittivity value and able to be compared together with the iFac ref. Based on the research done, it can be shown that increasing the temperature causes a consistent increase in permittivity [44].

3.4.1   Double boiled

The phantom mixture is put into a container and then double-boiled by being immersed in boiling water. This makes it possible to heat the mixture gradually and uniformly throughout. To achieve consistent phantom qualities, a fixed temperature must be maintained for a predetermined amount of time.
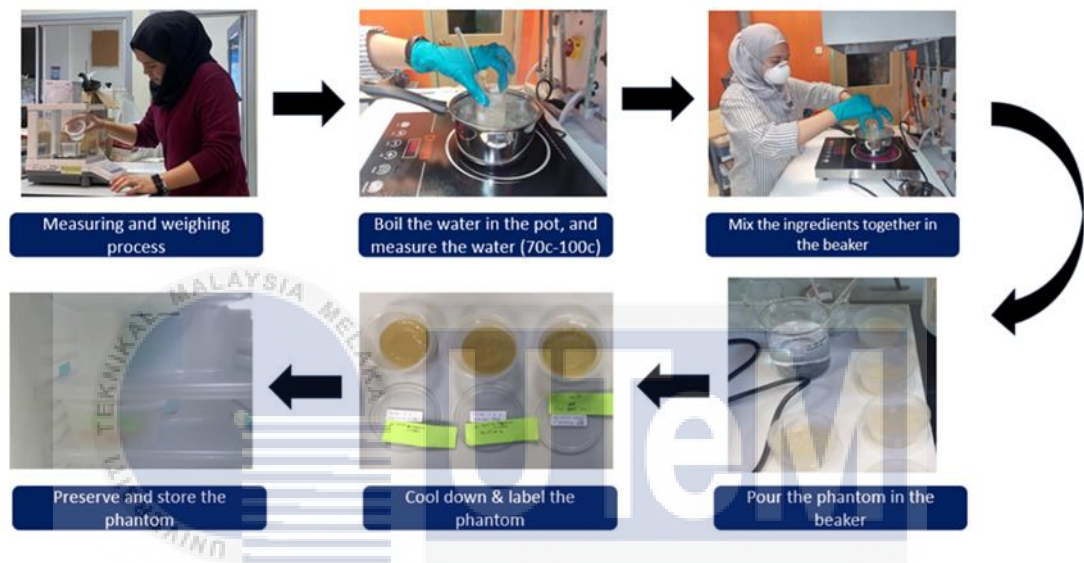
Figure 3.2: Tissue equivalent phantom development (double boiled) method

3.4.2   Direct heating

The phantom mixture is placed directly in a pot on an induction cooker using the direct heating technique; in contrast, the induction cooker employs electromagnetic fields to heat the contents of the pot quickly and effectively.
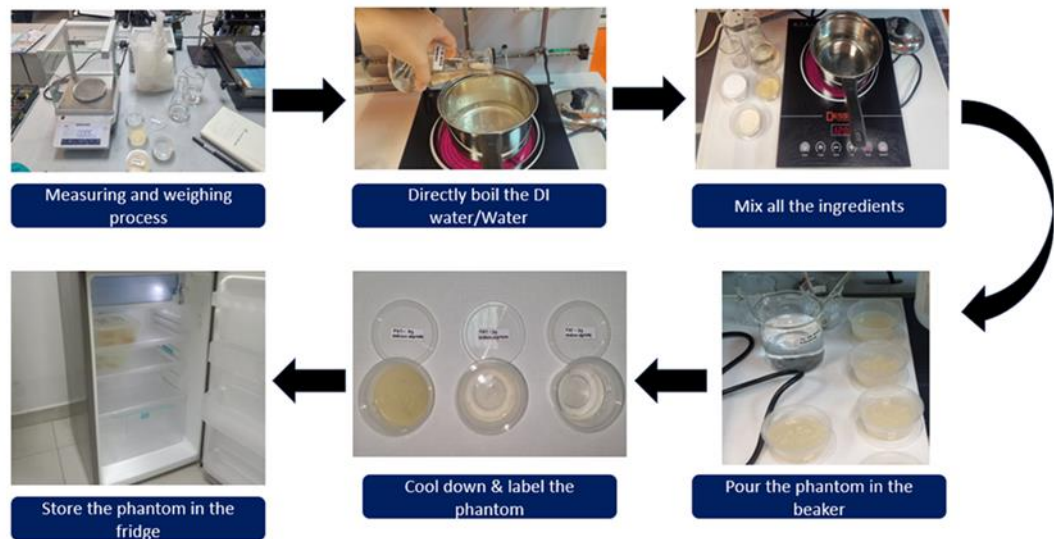
Figure 3.3: Tissue equivalent phantom development (direct heating) method

3.5   Dielectric properties measurement

The method of determining the electrical properties of materials that may store energy when an external electric field is applied is known as dielectric property measurement. Accurate dielectric property measurements can provide information for incoming inspection, process monitoring, and quality assurance. There are several ways to measure dielectric characteristics, each with its restrictions, such as transmission lines, open-ended coaxial probes, free space, and resonant approaches. In this research the performance probe is used to measure the permittivity and loss tangent of the tissue-equivalent phantom (MUT) [45].

The tissue equivalent phantom is positioned in the measurement setup, which usually entails sandwiching it in between the performance probe and the VNA. To test the phantom's electromagnetic characteristics, the probe is positioned to contact its surface.

1. Calibration: The VNA and performance probe need to be calibrated before measurements are made on the tissue equivalent phantom. Accurate measurements are made possible by the calibration process, which considers the natural losses and reflections in the measurement apparatus.

2. Measurement Method: Electromagnetic waves produced by the VNA are transferred into the tissue equivalent phantom via the performance probe. The waves interact with the phantom, and the VNA measures the reflected and transmitted waves.

3. The technician will open the probe and check that it has all the necessary parts, including the high-temperature dielectric probe, calibration short, and performance dielectric probe.

4. Utilizing an Agilent Technologies N5242A network analyzer, connect the probe to the PORT 1 on the analyser. To guarantee the accuracy of the results, calibrate by using the calibration brief that came with the probe to run a one-port calibration on the network analyser and test it on DI water as it acts as the neutralizer, before testing it on the tissue phantom.

3.5.1 Measurement setup
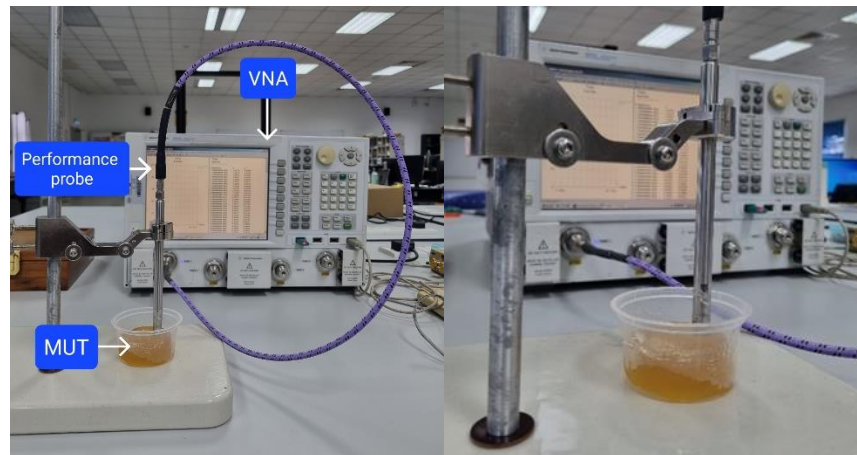
Figure 3.4: Shows the measurement setup consisting of the performance probe, vector network analyzer and the tissue-equivalent phantom as the (MUT).

Vector Network Analyzer: An electronic device known as a vector network analyser (VNA) is used to measure the electrical properties of high-frequency components and circuits. It works by sending and receiving electromagnetic waves to examine the sample measure's qualities for reflection and transmission [46].

Keysight *85070E Dielectric Probe Kit* (Performance Probe): A performance probe is a specialized probe that is utilized with VNA. It is designed to make exact measurements of the electromagnetic properties of the sample.

In materials testing, the sample or specimen that is being examined or assessed is referred to as the "material under testing" (MUT). The term "material under testing" describes a sample or specimen that is being examined or tested under different circumstances. The appropriateness of materials for different purposes can be ascertained using the outcomes of materials testing. In this research, the MUT is the developed tissue-equivalent phantom based of eco-friendly ingredients in development for biomedical microwave application.

Data analysis: The tissue equivalent phantom's dielectric characteristics are derived using the measured data from the VNA. The permittivity (also known as relative permittivity or dielectric constant) and conductivity of the material can be calculated through studying the reflection and transmission coefficients.

3.5.2 Calibration process for VNA and Performance probe

Calibration is setting up a measurement apparatus to generate results within a recognized range to reduce measurement errors. For precise measurement results, vector network analysers (VNAs) and performance probes must be calibrated. Furthermore, calibration is essential to remove mistakes from the measuring process, such as zero or large faults brought on by the measuring apparatus. Findings can be more accurate if these errors are recognized and described. By employing a mathematical method known as vector error correction to calibrate the test device, VNAs offer extremely accurate measurements. This kind of calibration considers measurement errors in the network analysers, fixtures, probes, test cables, and adapters.

For this reason, calibration is necessary to ensure the accuracy and consistency of the data obtained from performance probes and VNAs. Short and load standards to the coaxial probe must be used to calibrate the performance probe and measured, followed by the probe's reaction to the brief standard. Next, measure established standards and compare the results to anticipated DI water and air readings to confirm the calibrated probe's accuracy.

Established calibration standards, such as short circuits, open circuits, and matched loads, are commonly connected to the VNA during calibration. The VNA can determine calibration coefficients or correction factors for each frequency point by

monitoring the responses to these standards, which have electrical characteristics that are clearly specified. Then, the following measurements are adjusted using these coefficients. By performing regular calibration, VNA users can achieve more accurate and repeatable measurements, enabling precise characterization and analysis of RF and microwave devices.
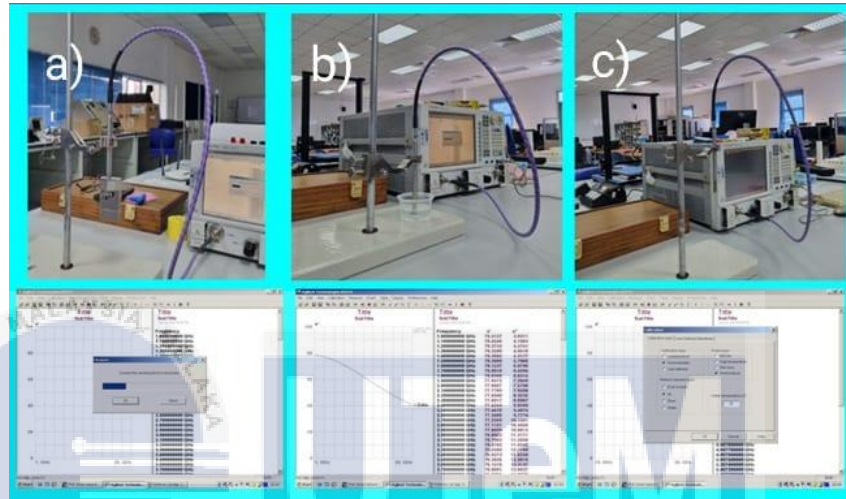
Figure 3.5: The calibration procedure includes a) air, b) water, and c) free space.

3.5.3   Tissue-Equivalent Phantom Measurement process

Once the tissue phantom had cooled down after the fabrication process, it was stored in the chemical refrigerator to prevent it from drying out and to avoid the growth of Mold. Keeping the phantom is an essential part of the process because maintaining it at room temperature can alter the dielectric properties, and the dielectric needs to be measured a few times within a time frame; in this research, the phantom is calculated within 14 days to analyse, the dielectric properties, the chemical properties, and the mechanical properties. Measuring the dielectric properties of the phantom was simple because no unique fixtures or containers are required, and measurements are non-

destructive [47]. Besides, it is also suitable for measuring semi-solid materials like the tissue phantom developed.

The network analyzer measures the material's response to microwave energy, where the probe transmits a signal into the Material Under Test (MUT). The results of the sample's measurement can be viewed in a range of formats namely ε,' ε "loss tangent [48]. As mentioned in the scope of work, the existence of the slim probe, an open-ended coaxial probe, was connected to a performance probe instead because it supports a wide range of temperatures –40 °C to 200 °C and is suitable to be used for semi-solid samples [49] [50]. Before the measurements were taken, the calibration process was done by configuring the calibration where the type of calibration was set to air short or water, and the probe type was set to performance. The water temperature was set to room temperature, 27 °C. Next, the range of frequency was set to 1GHz–20 GHz, and performance calibration was selected. The lens of the performance probe was cleaned before deciding 'OK' for the performance probe to be left in open air.

The shorting block was connected to the probe, and 'OK' was selected. The shorting block was removed, and a cup of water was inserted into the probe and clicked 'OK.' The sample was measured by placing the performance probe on the surface of the phantom and measured on multiple locations to ensure the dielectric values were almost similar to each other; this due to the bubble on the tissue phantom developed are still there, therefore avoiding "loss" or inaccuracy the data were taken 3 times every time the measurement was taken. Each of the data will be saved as "memory1", "memory 2," and "memory 3." Later, the average of the measurements will be taken.

CHAPTER 4

RESULTS AND DISCUSSION

This chapter presents the results and analysis of the tissue equivalent phantom acquired spanning the frequency range of 1GHz to 20GHz. Tissue-comparable phantom samples were constructed for each type of tissue based on human anatomical parameters that match the actual human tissue dielectric properties, which are relative permittivity and loss tangent. Each of the samples created is compared using non-eco-friendly based ingredients phantom, environment-friendly based ingredients phantom, and human tissues. Some data are gathered from previous papers to analyse the best sample in relative permittivity and loss tangent. Based on the data collected throughout the semester, the measurements and data collection are kept in an Excel file and plotted into a graph to be compared together. Each of the samples is tested from time to time

for up to 14 days to study the trend of the graph to ensure the durability and the quality of the tissue phantoms.

4.1 Result and analysis of skin tissue phantom

The development of the skin tissue phantom has been divided into two categories: non-ecofriendly based (RED) and eco-friendly (GREEN) ingredients. The non-ecofriendly tissue-equivalent phantom is developed to study the base ingredients that can be reused to replicate the recipe from the non-ecofriendly tissue phantom for the eco-friendly skin tissue-equivalent phantom. The bold ingredients the non-ecofriendly materials

4.1.1 Recipe of non-ecofriendly vs. eco-friendly skin phantom

Table 4.1 recipe of non-ecofriendly vs. eco-friendly skin phantom

Ingredients (gram)	Non-eco skin 1	Non-Eco skin 2	Non-eco skin 3	Eco skin 1	Eco skin 2	Eco skin 3	Eco skin 4	Eco skin 5
PEP	10.67	-	-	-	-	-	-	-
Glycerine	-	19.16	19.16	-	-	-	-	-
Deionized water (DI)	50	70	70	100	100	100	100	100
Plant based glycerine	-	-	-	-	-	-	5	-
Plant-based Glycerine	-	-	-	-	-	-	5	-
Maltodextrin	-	12.13	12.13	-	-	-	-	-
Gelatine	-	6.93	6.93	10	10	10	20	30
Sodium benzoate	-	0.17	0.17	-	-	-	-	-
PDV Salt	-	1.04	0.9	5	5	2.5	2.5	2.5
Xanthan gum	0.67	-	-	3	1	3	-	-
Agar	1.57	-	-	-	-	-	-	-
Soy lecithin	-	-	-	3	-	2	-	2
PVP K-90	-	-	-	-	6	-	-	-
Sugar	-	-	-	-	2.5	-	2.5	5
Carrageenan gum	-	-	-	-	-	-	10	-

Table 4.1 shows the comparison of recipe of non-ecofriendly and eco-friendly skin tissue-equivalent phantom. The research aims to develop an eco-friendly skin tissue phantom by comparing three non-eco-friendly phantoms with five eco-friendly alternatives. This involves a comprehensive analysis of the ingredients used in the phantoms, drawing on previous studies and citations. The objective is to characterize eco-friendly ingredients for developing tissue-equivalent phantoms while ensuring the exclusion of non-eco-friendly components. This comparative approach will facilitate the gradual assessment of the developed phantoms, ultimately identifying the best-suited eco-friendly skin tissue phantom.

4.1.2 Dielectric properties of skin tissue phantom
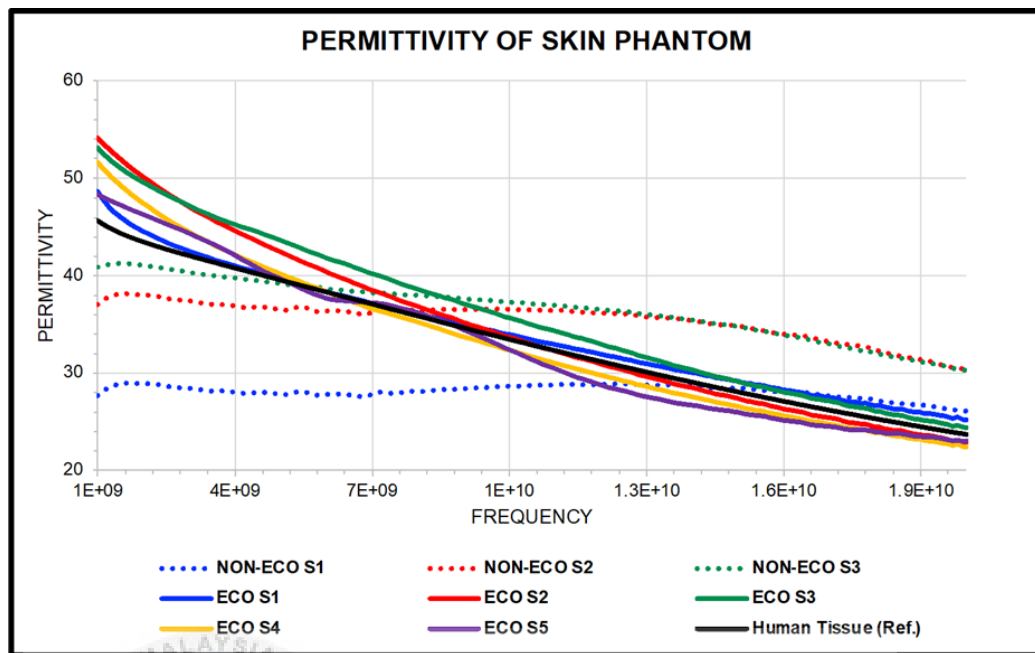
Figure 4.1: Relative permittivity of skin tissue phantom
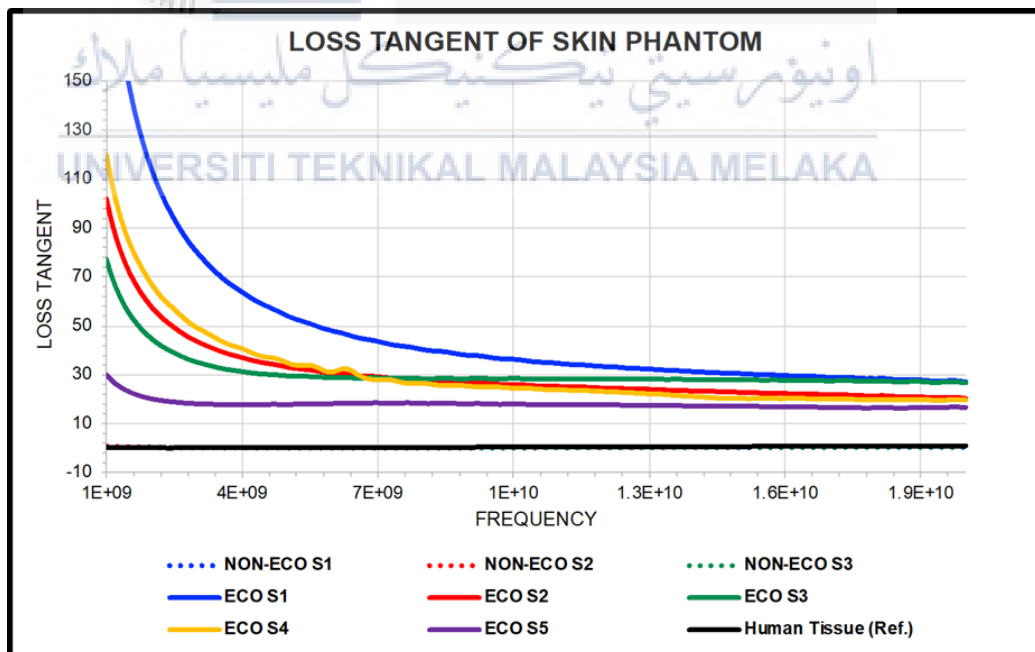
Figure 4.2: Loss tangent of skin tissue phantom

The graph of dielectric properties; relative permittivity shows that eco-friendly-based ingredients for skin tissue phantoms are comparable to human skin tissue, with only slight differences in the graph trend. Table 4.2 below states that the relative permittivity and loss tangent were compared at 2.4GHz and 5.8GHz. While no relevant search results were found on the eco-friendly and biodegradable tissue-equivalent phantom, the graph and table prove the relevance of the eco-friendly tissue phantom. These studies emphasize the importance of understanding sustainable compounds' chemical and physicochemical properties to predict stability, performance, mechanical properties, and, most importantly, dielectric properties. It is also crucial to select sustainable raw materials based on their biodegradability pattern, bio-based composition, origin, and source. These studies provide valuable insights into the importance of eco-friendly and sustainable ingredients in biomedical engineering.

Table 4.2: Comparison table for Eco-friendly based ingredients for muscle tissue equivalent phantom in terms of relative permittivity and loss tangent at 2.4GHz and 5.8GHz

Tissues	Frequency= 2.4GHz		Frequency= 5.8 GHz	
	Permittivity	Loss tangent	Permittivity	Loss tangent
ECO S1	43.6163	97.0996	38.6462	48.9728
ECO S2	48.8251	50.6145	40.8492	31.1239
ECO S3	48.5594	39.846	42.2103	28.9983
ECO S4	46.1309	58.3615	38.7404	31.7477
ECO S5	45.5087	18.954	38.0325	17.984
HUMAN REF.	42.923	0.24191	38.0325	0.31715

Table 4.2 shows the comparison of permittivity & loss tangent for diff. tissue phantom developed (eco-friendly for skin phantom) at 2.4 GHz and 5.8 GHz. ECO S1 was selected as the closest to mimicking the human skin tissue, and will also be used in analysis of time, recent paper.

4.1.3   The effect of ingredients on skin tissue phantom

Table 4.3: The study effects of salt, sugar and gelatine in skin tissue phantom

	Salt	Sugar	Gelatin
Texture	↑ = *no effect* ↓ = no effect	↑ = *no effect* ↓ = no effect	↑ = *Elastic* ↓ = less elasctic
Permittivity	↑ = *high* ↓ = low	↑ = *high* ↓ = low	↑ = *high* ↓ = low
Loss tangent	↑ = *high* ↓ = low	↑ = *high* ↓ = low	↑ = *high* ↓ = low

Based Table 4.3, the recipe developed, some of the ingredients were repeated. Still, slight changes were made in the measurement to study the effect of the ingredients on the tissue phantom in terms of structure, relative permittivity, and loss tangent.

This research found that as the salts are increased, the texture will show no changes on the skin tissue phantom; this also goes when the number of salts is decreased. However, the relative permittivity of the skin tissue phantom shows that the skin trend will increase but still be stable and maintained at a reasonable value and vice versa. The studies on salt also found that the loss tangent increased drastically when the relative permittivity was increased. However, it should be noted that the ratio of the imaginary and real parts of the relative permittivity is then the loss tangent [51]. Therefore, decreasing the amount of salt will reduce the number of the loss tangent on the skin tissue phantoms.

Sugar plays almost a similar role as salt in increasing the permittivity, and it does not change the structure of the skin tissue phantoms. Instead, it increases the relative permittivity and the loss tangent of the skin tissue phantom; hence, when the amount

of sugar is decreased, the relative permittivity is reduced, and the loss tangent is also reduced.

Gelatine is the most common ingredient used in this skin tissue development since both non-ecofriendly based and eco-friendly skin tissue phantom use gelatine to create a texture where that can be flexible, elastic, and malleable according to the number of gelatines used and mixed with other ingredients. In terms of relative permittivity, as the amount of gelatine used is increased, the relative permittivity of the skin tissue phantoms is also increased. The same goes for the loss tangent of the skin tissue phantom, where the gelatine use will have a huge impact on the loss tangent as well as its other dielectric properties.

4.1.4 Time analysis of the skin tissue phantom within 14 days

4.1.4.1 Time analysis of relative permittivity of skin tissue phantom
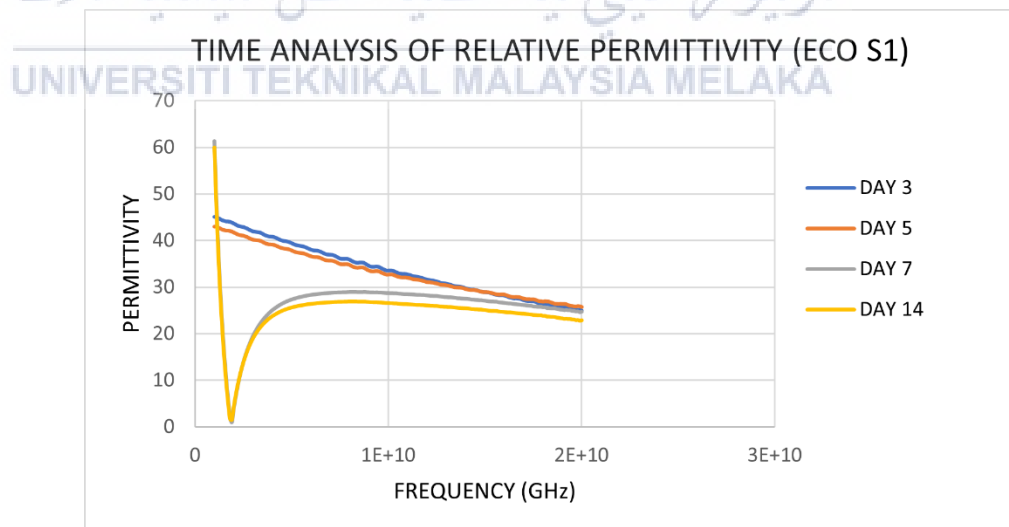
Figure 4.3: Time analysis of relative permittivity ECO S1

Based on the graph time analysis of relative permittivity for ECO S1, it can be seen that from day three until day 5, the graph shows consistency and is still stable to be

used. However, after seven days, the phantom decreases performance in the relative permittivity value. After 14 days, it can be seen that the graph starts to show an unreasonable trend on the graph. It can be considered a phantom that cannot perform according to the best relative permittivity compared to the human skin.
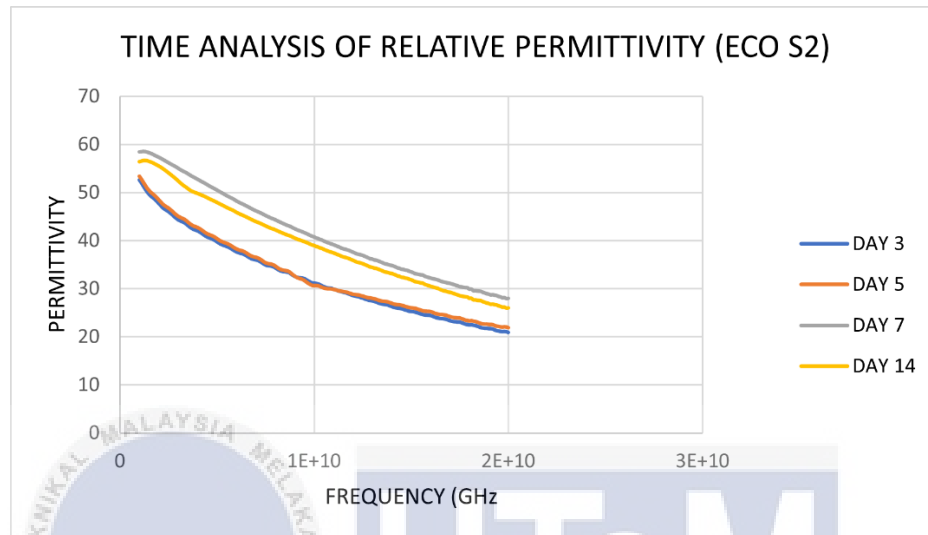
Figure 4.4: Time analysis of relative permittivity ECO S2

ECO S2 time analysis in 14 days shows the consistency in the trend on the graph, from day 3 until day 5, with a slight decrease in the relative permittivity performance. However, from day seven until day 14, the graph shows the relative permittivity value increased compared to day five and day 7.
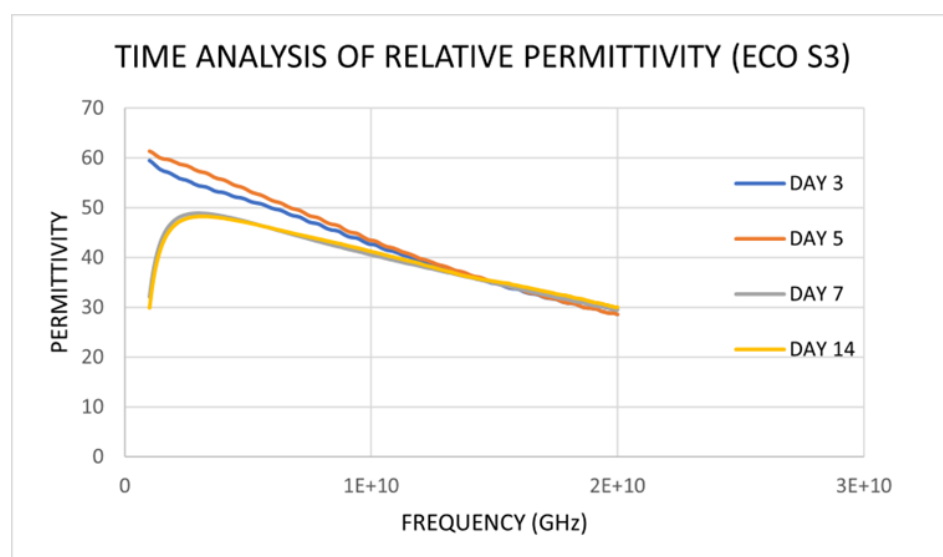
Figure 4.5: Time analysis of relative permittivity ECO S3

According to the graph time analysis of the relative permittivity of ECO S3, It can be seen the consistency taken on day five and day 7, where the relative permittivity started to increase on the value but still maintains the consistency where it does not show a considerable gap and differences.
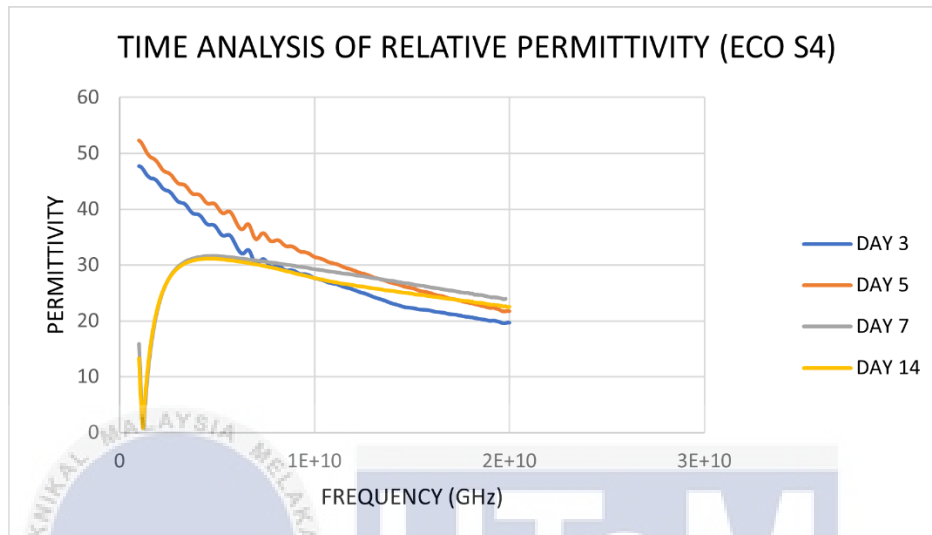
Figure 4.6: Time analysis of relative permittivity ECO S4

The ECO S4 skin phantom shows the most inconsistent graph trend, where on day three and day 5, the fluctuation on the graph can be seen. On day seven and day 14, the graph starts to show the inverse proportion of the graph, and the skin phantom can be considered irrelevant to be compared with human skin tissue.
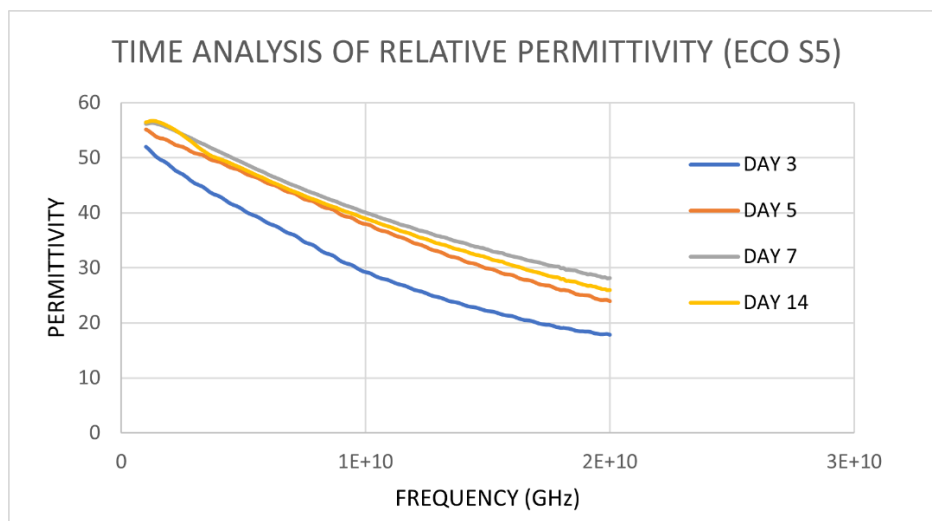
Figure 4.7: Time analysis of relative permittivity ECO S5

The ECO S5 skin phantom is also one of 5 skin tissue phantoms that shows the best trends in terms of consistency to keep the trends directly proportional. After day 3, day 5, day seven and day 14, the graph can remain consistent and show a manageable graph trend gap.

4.1.4.2 Time analysis of loss tangent of skin tissue phantom
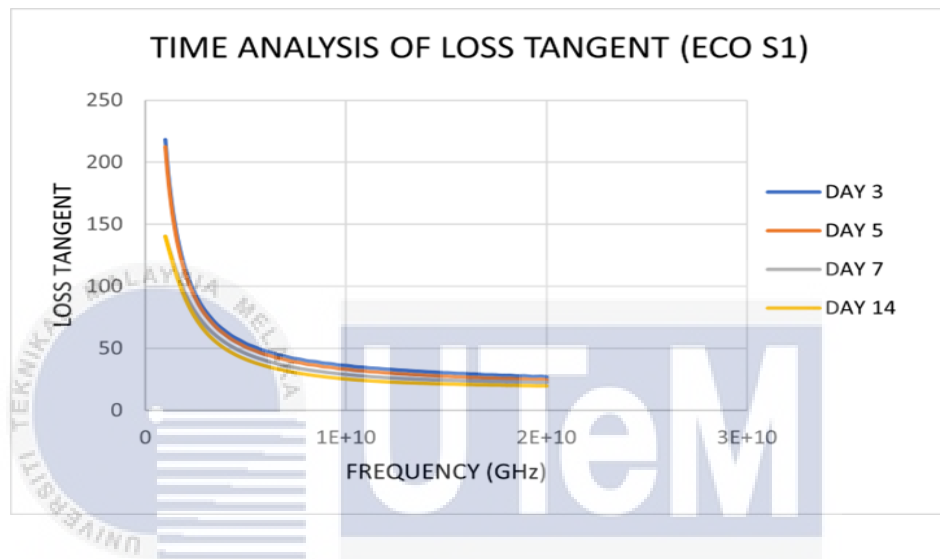
Figure 4.8: Time analysis of loss tangent ECO S1
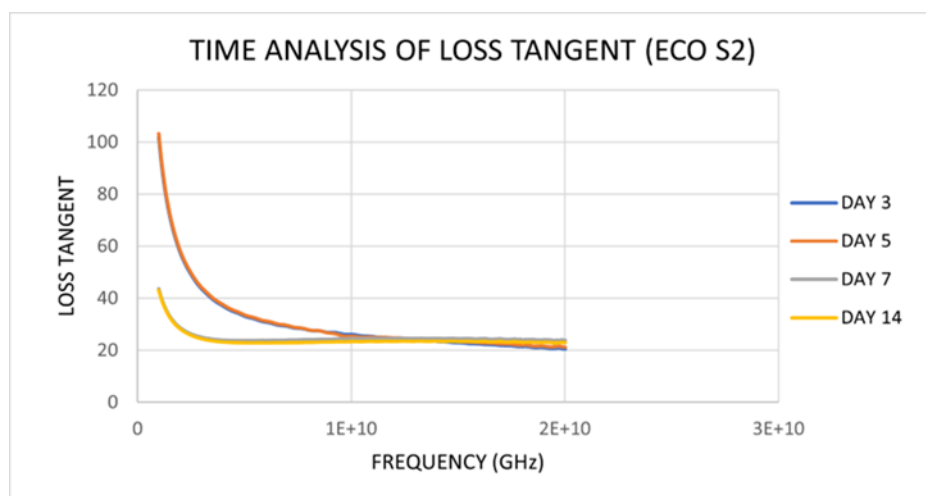
Figure 4.9: Time analysis of loss tangent ECO S2
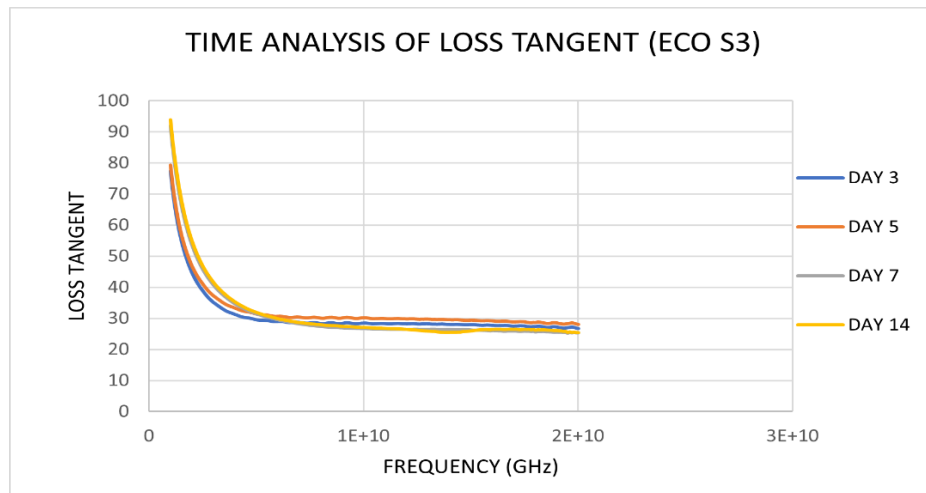
Figure 4.10: Time analysis of loss tangent ECO S3
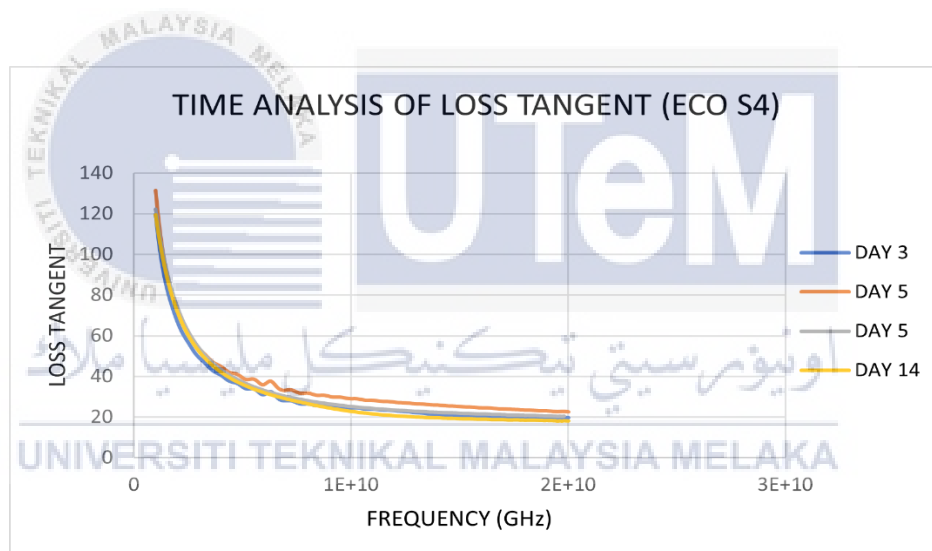
Figure 4.11: Time analysis of loss tangent ECO S4
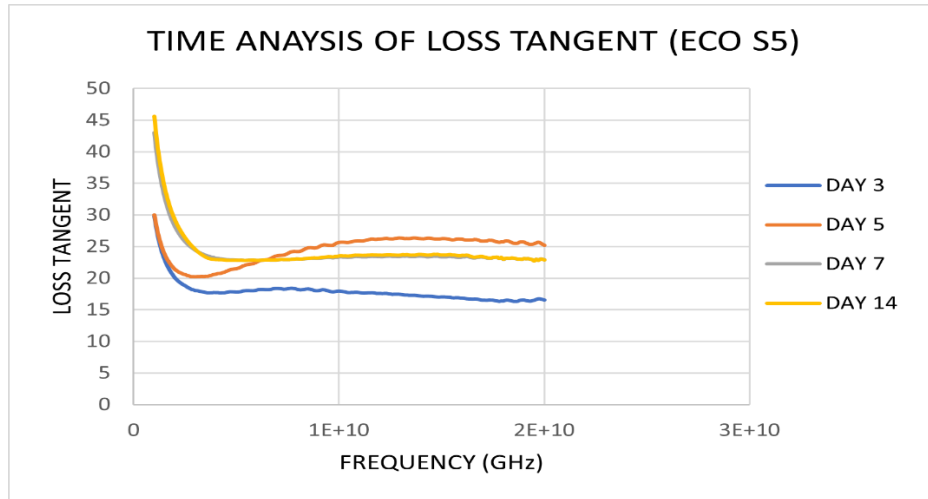
Figure 4.12: Time analysis of loss tangent ECO S5

4.2 Result and analysis of fat tissue phantom

The development of the fat tissue phantom was divided into two categories: non-ecofriendly (RED) and eco-friendly (GREEN) ingredients. The non-ecofriendly tissue-equivalent phantom was created to investigate the base ingredients that can be reused to recreate the recipe from the non-ecofriendly tissue phantom for the eco-friendly fat tissue-equivalent phantom. The materials that are non-ecofriendly were written in bold.

4.2.1 Recipe of non-eco-friendly vs. eco-friendly fat phantom

Table 4.4: Recipe of non-eco-friendly vs. eco-friendly fat phantom

Ingredients (gram)	Non-eco fat 1	Non-Eco fat 2	Non-eco fat 3	Eco fat 1	Eco fat 2	Eco fat 3	Eco fat 4
Kerosene	15.9	15.9	-	-	-	-	-
N-propanol	-	6.22	-	-	-	-	-
PEP	-	-	10.67	-	-	-	-
Canola oil	15	15	-	-	20	-	-
Glycerine	20	20	-	-	-	-	-
Deionized water (DI)	10.9	10.9	50	100	100	100	100
Plant based glycerine	-	-	-	35	35	35	100
Gelatine	6	6	-	-	-	-	-
PDV Salt	0.3	0.3	-	10	30	20	3
Hydroxyethyl cellulose	-	-	1.53	-	-	5	-
Agar	-	-	1.57	-	-	-	-
Sodium alginate	-	-	-	5	-	-	2
Sodium benzoate	-	-	-	10	10	-	-
Xanthan gum	-	-	-	-	-	-	-
Guar gum	-	-	-	-	-	-	-

According to Table 4.4 , the study aims to create an eco-friendly fat tissue phantom by comparing three non-eco-friendly phantoms to four eco-friendly alternatives. This

involves thoroughly examining the chemicals employed in the phantoms based on past research and sources. The goal is to characterize eco-friendly substances for producing tissue-equivalent phantoms while guaranteeing that non-eco-friendly ingredients are excluded from developing eco-friendly tissue phantoms. This comparative technique will allow a more gradual evaluation of the produced phantoms, eventually identifying the best-suited eco-friendly fat tissue phantom.

4.2.2 Dielectric properties of fat tissue phantom
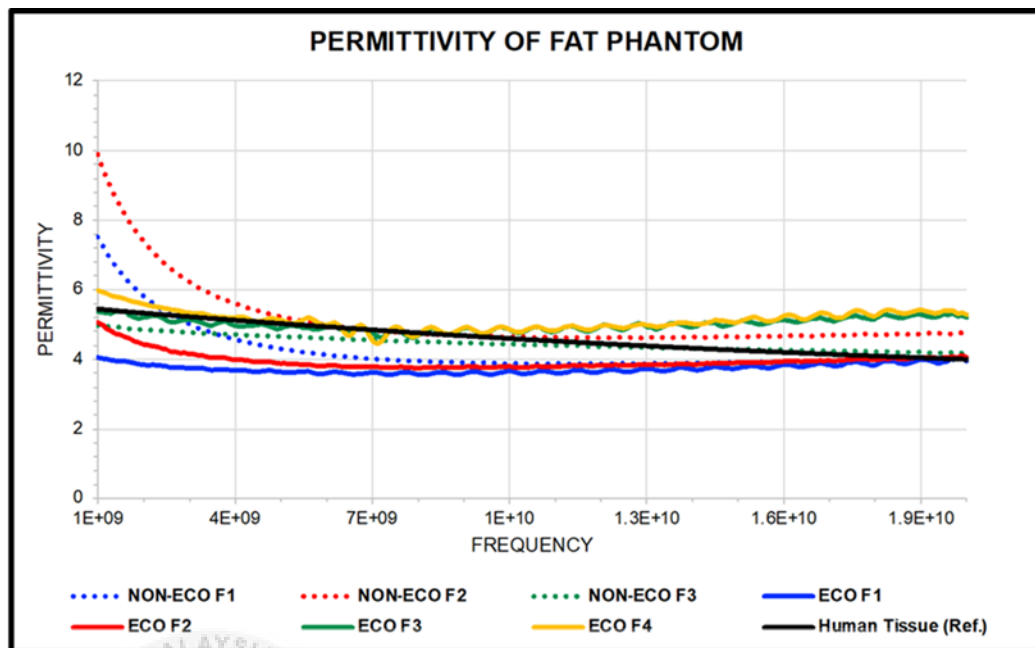
Figure 4.13: Relative permittivity of fat phantom
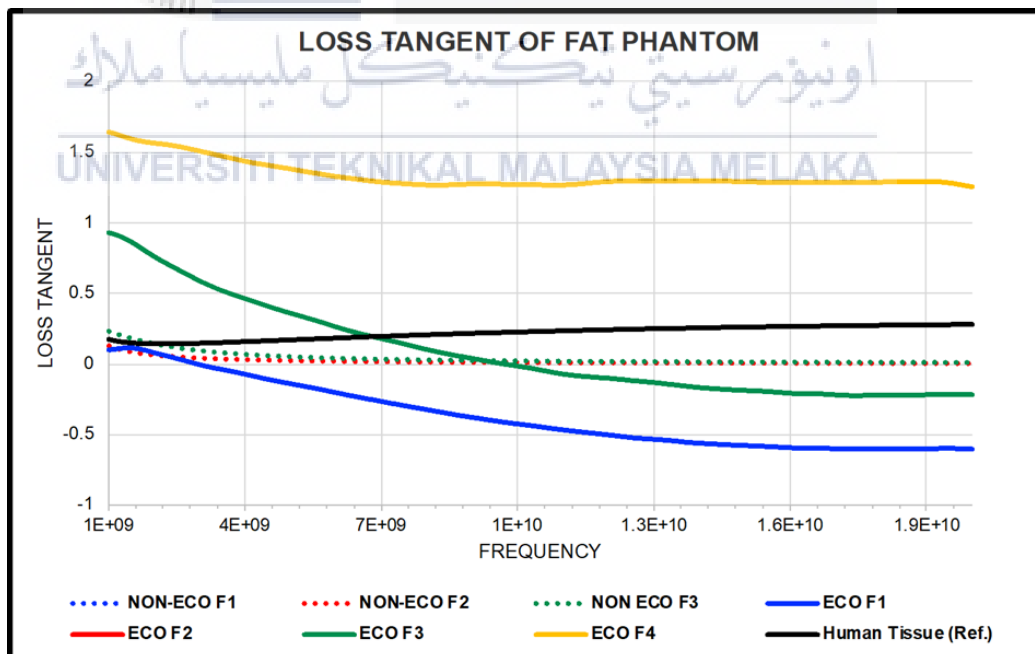
Figure 4.14: Loss tangent of fat phantom

The relative permittivity graph of dielectric characteristics demonstrates that the eco-friendly-based ingredients used in fat tissue phantoms are similar to human fat tissue, with just minor variations in the graph's overall trend. At 2.4GHz and 5.8GHz, the relative permittivity and loss tangent were evaluated. The eco-friendly and biodegradable tissue-equivalent phantom did not yield any relevant search results; however, the graph and table demonstrate the phantom's relevance. This research highlight the significance of comprehending the physicochemical and chemical features of sustainable chemicals in order to forecast mechanical, dielectric, performance, and stability properties. A sustainable raw materials origin, source, biobased composition, and biodegradability pattern must all be taken into consideration. This research provide useful insights about the importance of eco-friendly and sustainable chemicals in biomedical.

Table 4.5: Comparison table for Eco-friendly based ingredients for fat tissue equivalent phantom in terms of relative permittivity and loss tangent at 2.4GHz and 5.8GHz

Tissues	Frequency= 2.4GHz		Frequency= 5.8 GHz	
	Permittivity	Loss tangent	Permittivity	Loss tangent
ECO F1	3.8075	0.0511	3.5697	--0.1892
ECO F2	4.3149	0.6862	3.8049	0.2778
ECO F3	5.6855	0.24885	5.2416	-0.1019
ECO F4	9.3386	1.56337	8.4762	1.2765
HUMAN REF.	5.2853	0.14503	4.9549	0.18335

The relative permittivity and loss tangent were investigated at 2.4GHz and 5.8GHz, as shown in Table 4.4.3. While there were no relevant search results for the eco-friendly and biodegradable tissue-equivalent phantom, particularly the fat phantom, the table compares relative permittivity and loss tangent. These studies stress the importance of understanding the chemistry and features of sustainable substances to

predict stability, performance, mechanical capabilities, and, most importantly, dielectric properties. Selecting sustainable raw materials based on their biodegradability pattern and bio-based content is also crucial. This study emphasized the importance of eco-friendly and sustainable materials in biomedical engineering.

4.2.3 Effect of ingredients on fat tissue phantom

Table 4.6: The study effects of canola oil, sodium benzoate and sodium alginate in fat tissue phantom.

FAT	Canola oil	Sodium benzoate	Sodium alginate
Texture	↑ = *oily* ↓ = less oily	↑ = *dry* ↓ = moist	↑ = *dry* ↓ = moist
Permittivity	↑ = *high* ↓ = low	↑ = *low* ↓ = high	↑ = *low* ↓ = high
Loss tangent	↑ = *high* ↓ = lower than without canola oil	↑ = *lowest* ↓ = high	↑ = *lowest* ↓ = high

Based on the developed recipe, some of the ingredients were repeated. However, minor adjustments were made in the measurements to investigate the impact of some of the ingredients on the tissue phantom in terms of structure, relative permittivity, and loss tangent.

It can be observed that the increased amount of canola oil in fat tissue development shows a very oily texture even though the phantoms are flexible; hence, decreasing the amount of canola oil will create a less oily or non-oily structure of fat tissue phantom. However, the increased amount of canola oil will affect the relative permittivity of the fat tissue phantom; the relative permittivity will increase, and so will the loss of tangent. Nevertheless, the range of the relative permittivity and the loss

tangent is still in the acceptable range and plotted nicely to be compared with the human fat tissue.

The sodium benzoate has a significant impact on the fat tissue phantom structure, where it will create a dry and malleable fat tissue phantom [52]. When the amount of sodium benzoate decreases, the texture of the fat tissue phantoms is moist compared to the one with sodium benzoate added. In terms of relative permittivity, as the amount of sodium benzoate increases, the relative permittivity decreases; the same goes for loss tangent; when the amount of sodium benzoate increases, the loss tangent will decrease according to the relative permittivity taken.

This research also measured and studied the amount of sodium alginate to be compared with other ingredients that may affect the relative permittivity, loss of tangent and structure, such as canola oil and sodium benzoate. As sodium alginate acts as the thickening agent and gelling agent [53], it has been observed that the structure of the fat tissue phantom created is dry, and sediments are formed on the fat tissue phantom. In the form of relative permittivity, the phantom with sodium alginate shows the number of relative permittivity was slightly lower compared to the one with no sodium alginate; as the number of sodium alginate was decreased or removed, the number of relative permittivity was higher. The same goes for the loss tangent; hence, when the number of sodium alginate increased, the loss tangent of the tissue phantom decreased.

4.2.4   Time analysis of fat tissue phantom in 14 days

4.2.4.1   The analysis of relative permittivity of fat tissue phantom in 14 days.
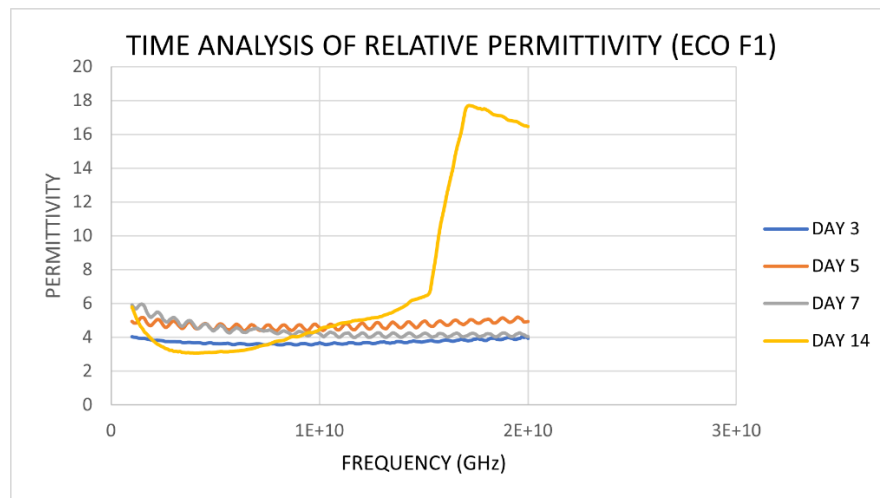
Figure 4.15: Time analysis of relative permittivity ECO F1

Based on the graph time analysis of relative permittivity for ECO F1, it can be seen
that from day three until day 7, the graph shows consistency and is still stable to use,
even though the relative permittivity obtained fluctuate. However, after seven days,
the phantom decreases performance in the relative permittivity value. After 14 days,
it can be seen that the graph starts to show an unreasonable trend on the graph. It can
be considered a phantom that cannot perform according to the best relative permittivity
compared to the human skin.
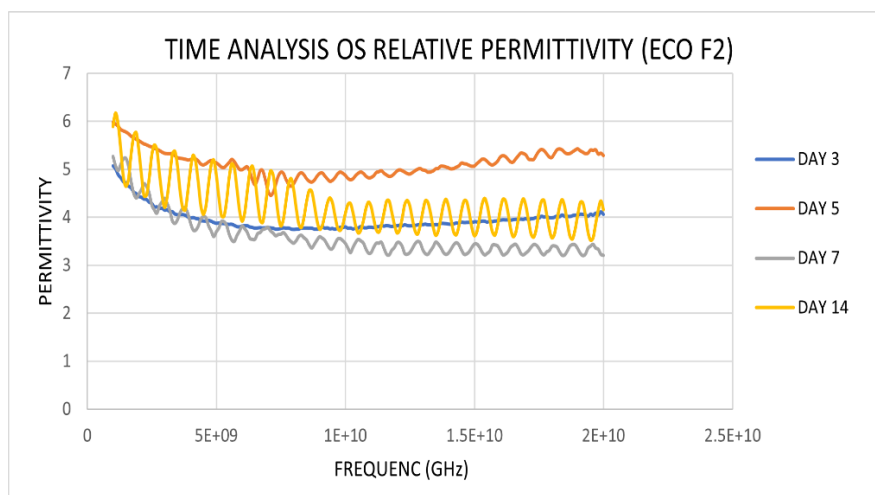
Figure 4.16: Time analysis of relative permittivity ECO F2

ECO F2 time analysis on day three shows a reasonable trend, up until day five, even with a slight fluctuation on the graph in 7 days; on day 14, the trend shows inconsistency in the trend on the graph, and the fluctuation of the graph can be seen in the relative permittivity performance. The graph is no longer stable and can be considered a less-performed phantom.
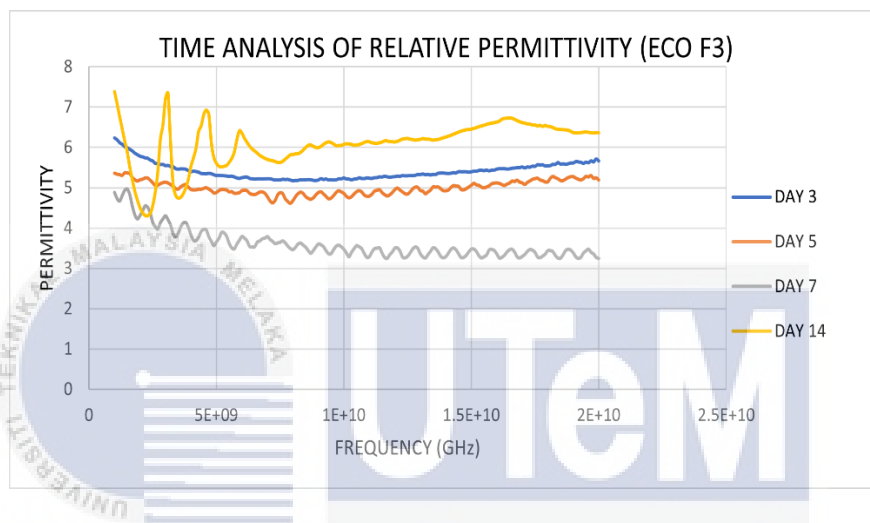
Figure 4.17: Time analysis of relative permittivity ECO F3

According to the graph time analysis of the relative permittivity of ECO F3, it can be seen the consistency taken on the day starts to decrease on day five and shows the fluctuation on day five and on day seven, where the relative permittivity starts to increase and shows a significant fluctuation on the value and did not maintain the consistency where it does shows are huge gap and differences. And the phantom can be considered broken.
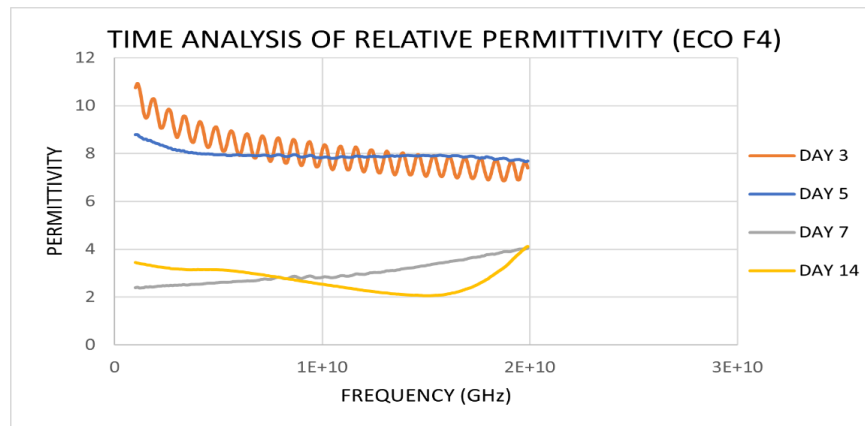
Figure 4.18: Time analysis of relative permittivity ECO F4

The ECO F4 fat phantom shows the most inconsistently in graph trend where on day three, the permittivity already started to significantly; on day 5, it shows that the phantom is regular in relative permittivity and on day 7, the fluctuation on the graph can no longer be seen, and on day 14 the graph starts to show the inversely in proportional of the graph and the skin phantom can be considered as not relevant to be compared with human skin tissue.

4.2.4.2   Time analysis of loss tangent of fat tissue phantom in 14 days
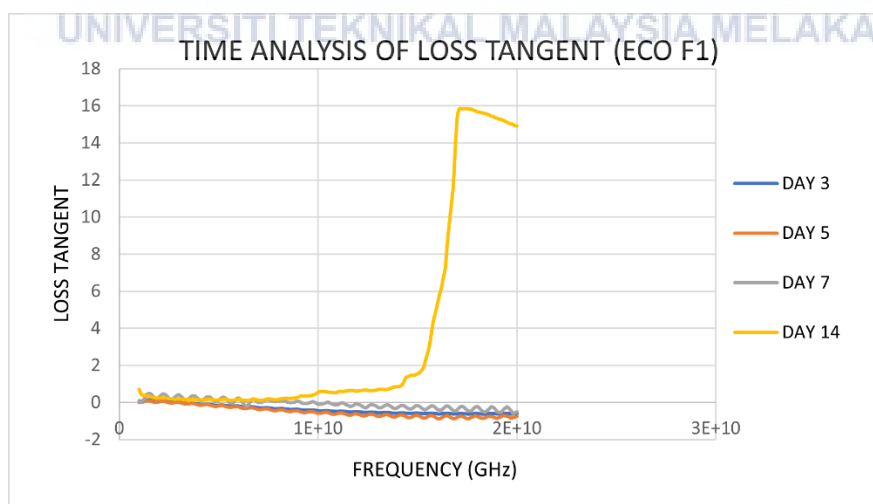
Figure 4.19: Time analysis of loss tangent ECO F1
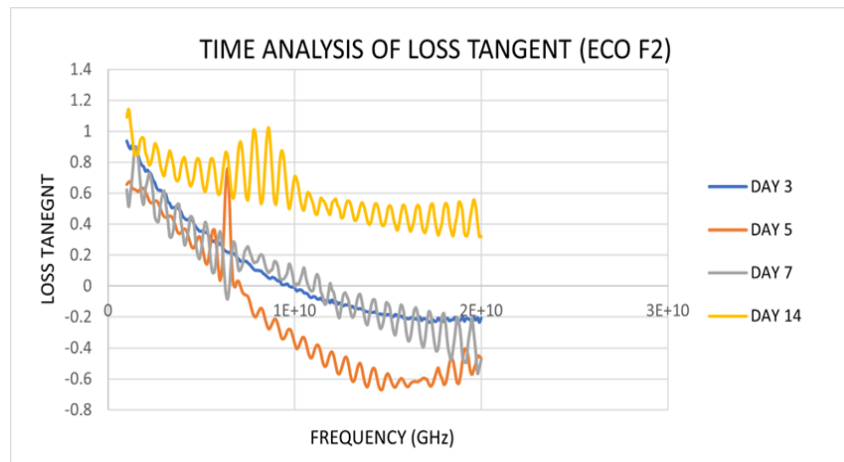
Figure 4.20: Time analysis of loss tangent ECO F2
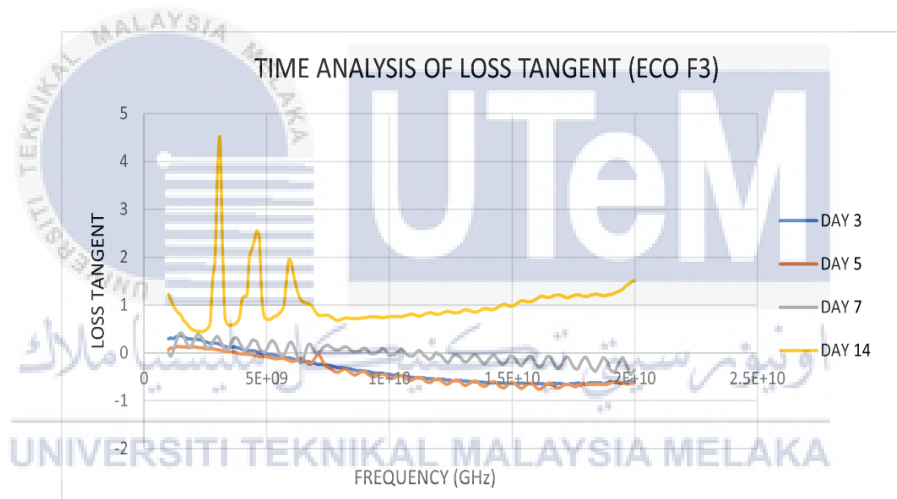
Figure 4.21: Time analysis of loss tangent ECO F3
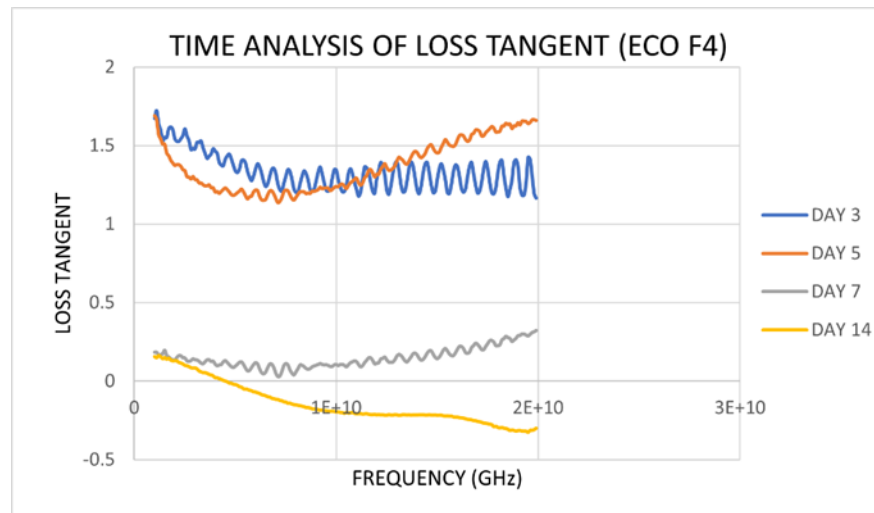
Figure 4.22: Time analysis of loss tangent ECO F4

4.3   Result and analysis of muscle tissue phantom

Materials that were used in the creation of the muscle tissue phantom were split into two categories: non-ecofriendly (RED) and eco-friendly (GREEN). The non-ecofriendly tissue phantom is created to investigate the base ingredients that can be reused to duplicate the recipe from the non-ecofriendly tissue phantom for the eco-friendly muscle tissue-equivalent phantom. The ingredients that are non-ecofriendly was written in bold.

4.3.1 Recipe of non-ecofriendly vs. eco-friendly muscle phantom

Table 4.7: Recipe of non-ecofriendly vs. ecofriendly muscle phantom

Ingredients (gram)	Non-eco muscle 1	Non-Eco muscle 2	Non-eco muscle 3	Eco muscle 1	Eco muscle 2	Eco muscle 3	Eco muscle 4	Eco muscle 5
PEP	10.67	10.67	10.67	-	-	-	-	-
Deionized water (DI)	50	50	50	100	100	100	100	100
Xanthan gum	0.67	-	-	2	5	2	-	-
Carrageenan gum	-	1.35	-	-	-	-	-	5
Agar	1.57	1.57	1.57	-	-	-	10	-
Guar gum	0.3	-	1.35	-	-	-	-	-
Gelatine	-	-	-	10	10	10	10	10
PDV salt	-	-	-	5	5	5	-	-
Soy lecithin	-	-	-	-	-	2	-	2.5
PVP K-90	-	-	-	-	2	-	-	-
Sugar	-	-	-	-	-	-	-	2.5
Plant based glycerine	-	-	-	-	-	-	10	5

Table 4.7 above states that the study compares three non-eco-friendly phantoms with five eco-friendly alternatives to build an eco-friendly muscle phantom. This involves a detailed analysis of the compounds used in the phantoms using previous studies and references. The objective is to identify environmentally friendly, biodegradable, and bio-compatible materials for creating tissue-equivalent phantoms while ensuring that non-eco-friendly components are not used to develop eco-friendly tissue phantoms. With this comparative technique, it will be possible to gradually evaluate the generated phantoms and ultimately determine which eco-friendly muscle tissue phantom is most appropriate.

4.3.2 Dielectric properties of muscle tissue phantom
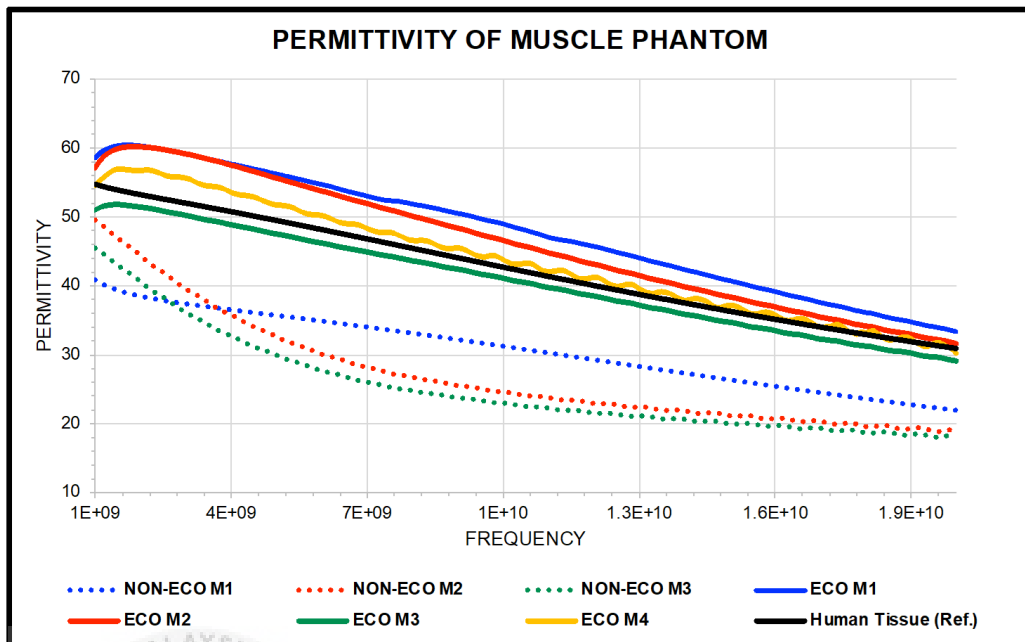
Figure 4.23: Relative permittivity of muscle tissue phantom
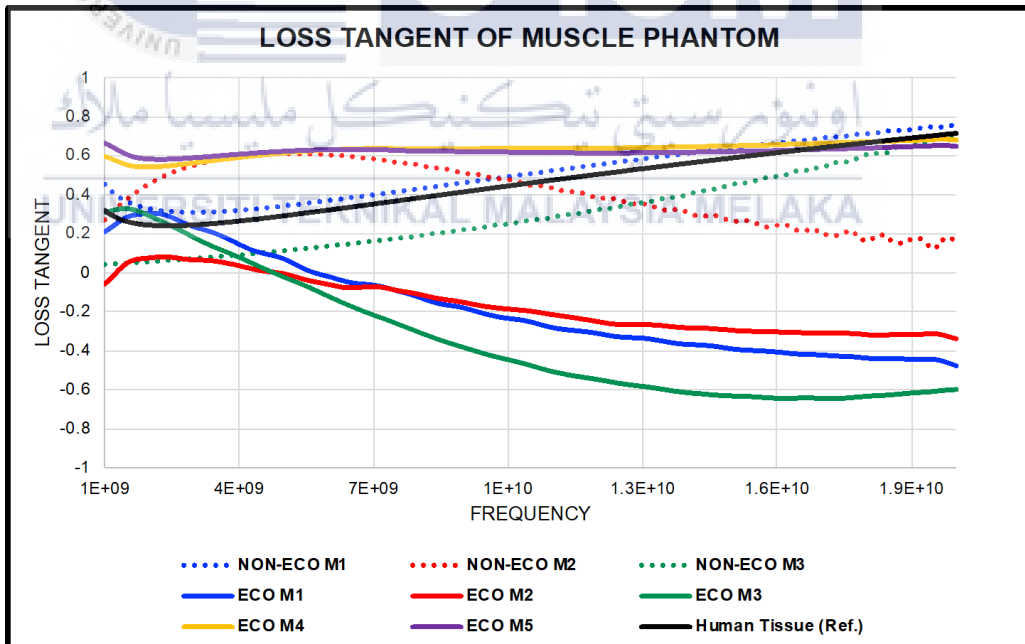
Figure 4.24: Loss tangent of muscle tissue phantom

The environmentally friendly components employed in muscle tissue phantoms are identical to human muscle tissue, as shown by the relative permittivity graph of dielectric properties, with only slight changes in the graph's trend. The relative permittivity and loss tangent at 2.4GHz and 5.8GHz were assessed using the following table. Although the eco-friendly and biodegradable tissue-equivalent phantom did not produce any pertinent search results, its importance is illustrated by the table and graph. This study emphasizes how critical it is to understand the molecular characteristics of sustainable chemicals to predict performance, stability, dielectric, and mechanical properties. It is necessary to consider the source, biocompatible basis, biodegradability pattern, and origin of sustainable raw materials. This study offers helpful information regarding the significance of sustainable and environmentally friendly chemicals in biomedical engineering.

Table 4.8: Comparison table for Eco-friendly based ingredients for muscle tissue equivalent phantom in terms of relative permittivity and loss tangent at 2.4GHz and 5.8GHz

Tissues	Frequency= 2.4GHz		Frequency= 5.8 GHz	
	Permittivity	Loss tangent	Permittivity	Loss tangent
ECO M1	59.9319	0.3146	55.0192	-0.0122
ECO M2	59.8731	0.109	54.1015	-0.0556
ECO M3	51.0209	0.2485	46.4689	-0.1019
ECO M4	52.3172	0.547372	46.1268	0.24737
ECO M5	57.3329	0.581499	49.935	0.626093
HUMAN REF.	52.791	0.24191	48.485	0.31715

According to Table 4.8, the relative permittivity and loss tangents were evaluated at 2.4GHz and 5.8GHz. The graph and table show the practicality of the eco-friendly and biodegradable tissue-equivalent phantom, even though no pertinent search results were obtained. These findings highlight the need to comprehend sustainable materials' physicochemical and chemical properties to predict mechanical performance,

stability, and, most importantly, dielectric properties. It's also crucial to choose sustainable raw materials based on their biodegradability pattern and percentage of biomass. This study clarified the importance of sustainable and environmentally friendly materials in biomedical engineering.

4.3.3   Effect of ingredients on muscle tissue phantom

Table 4.9: The study effects of PVP K-90, Soy lecithin and Xanthan gum in fat tissue phantom

MUSCLE	PVP K-90	Soy lecithin	Xanthan gum
Texture	↑ = *silky* ↓ = rough	↑ = *oily* ↓ = no oily	↑ = *slimy* ↓ = no slimy
Permittivity	↑ = *high* ↓ = low	↑ = *lower* ↓ = higher	↑ = *higher* ↓ = lower
Loss tangent	↑ = *high* ↓ = low	↑ = *lowest* *(negative)* ↓ = high	↑ = *high* ↓ = low

Based on the developed recipe, some of the ingredients were reused. However, some adjustments were made in the measurements to investigate the impact of some ingredients on the tissue phantom in terms of structure, relative permittivity, and loss tangent. Three ingredients were studied to compare the texture, relative permittivity, and loss tangent.

This research found that the PVP K-90 showed a smooth, silky texture, while the phantom developed without PVP K90 showed a rough texture but was still flexible and elastic. Regarding permittivity, it shows that relative permittivity is higher than without PVP K-90. However, the loss tangent remained higher, too. As the PVP K-90 decreases, the relative permittivity, and the loss tangent decrease.

Furthermore, the amount of soy lecithin added varies, and one of the recipes with soy lecithin was studied to determine the texture. It was found that the texture was a bit oily compared to muscle tissue without soy lecithin. However, the relative permittivity trend shows that the permittivity was lower than the muscle tissue without soy lecithin. Hence, the number of relative permittivity was quiet, the loss tangent showed the most downtrend, and it hit negative values.

Xanthomonas bacteria digest glucose, sucrose, or lactose to generate xanthan gum, a polysaccharide. It is employed as a thickening agent. Although stable over a broad pH and temperature range, excessive shear rates can affect the gel's elasticity and viscosity [54]. The texture of tissue muscle phantom with xanthan gum is slimy compared to the one with no xanthan gum in the developed muscle phantom. In terms of relative permittivity, the trend shows the permittivity is higher compared to the phantoms with no xanthan gum available in the developed tissues, and it was lower in no xanthan gum content, and the loss tangent higher with the availability of the xanthan gum and the loss tangent is lower too.

4.3.4   Time analysis of muscle tissue phantom in 14 days

4.3.4.1   The analysis of relative permittivity of muscle tissue phantom in 14 days
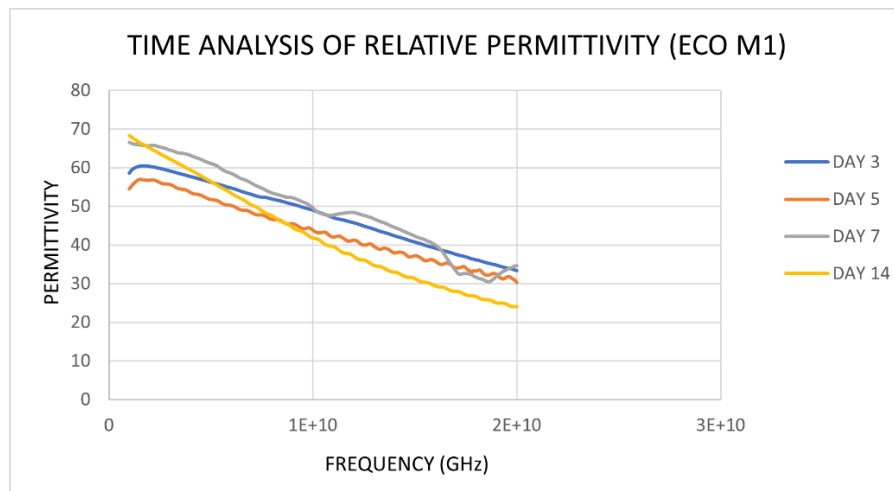
Figure 4.25: Time analysis of relative permittivity of ECO M1

Based on the graph time analysis of relative permittivity for ECO M1, it can be seen that on day 3, the graph shows a good trend. Still, it does not maintain consistency on day 7, where the graph is not smooth enough and fluctuates and on day seven, the graph shows unreasonable data. Some permittivity at specific frequencies starts to drop and is inconsistent compared with human muscle tissue, and it drops drastically on day 14. The ECO M1 muscle phantom cannot perform according to the best relative permittivity compared to the human skin after 14 days.
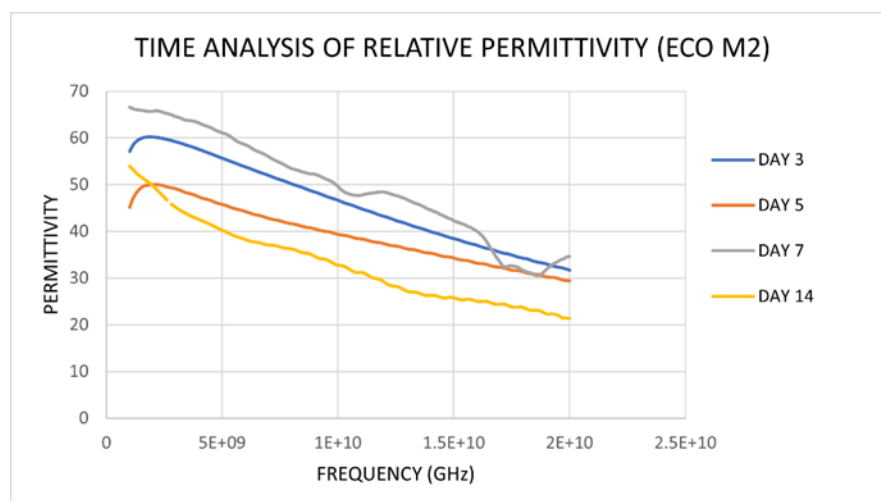
Figure 4.26: Time analysis of relative permittivity of ECO M2

ECO M2 time analysis in 14 days shows the consistency in the trend on the graph, from day three until day 5, with a slight decrease in the relative permittivity performance. However, from day seven until day 14, the graph shows the relative permittivity value increased on day seven and dropped drastically compared to day 14. The graph trend does not establish an apparent fluctuation; however, the performance of the relative permittivity has fallen.
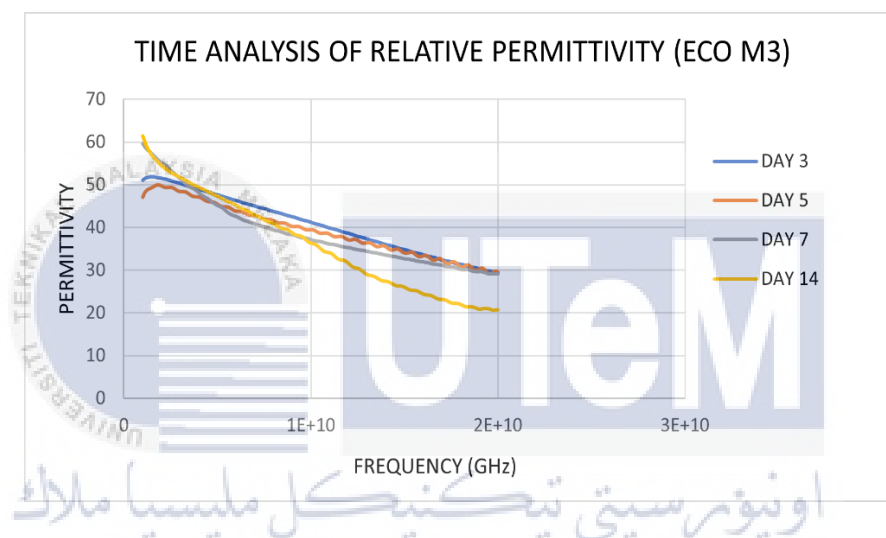
Figure 4.27: Time analysis of relative permittivity of ECO M3

According to the graph, time analysis of the relative permittivity of ECO M3 can be seen in the consistency taken on day three, followed by day five and day 7, with a slight drop and fluctuation in the relative permittivity value on day 14 where the relative permittivity started to decrease on the value but still maintains the consistency where it does show a considerable gap and differences, and the performance of the relative permittivity is acceptable at specific frequency range.
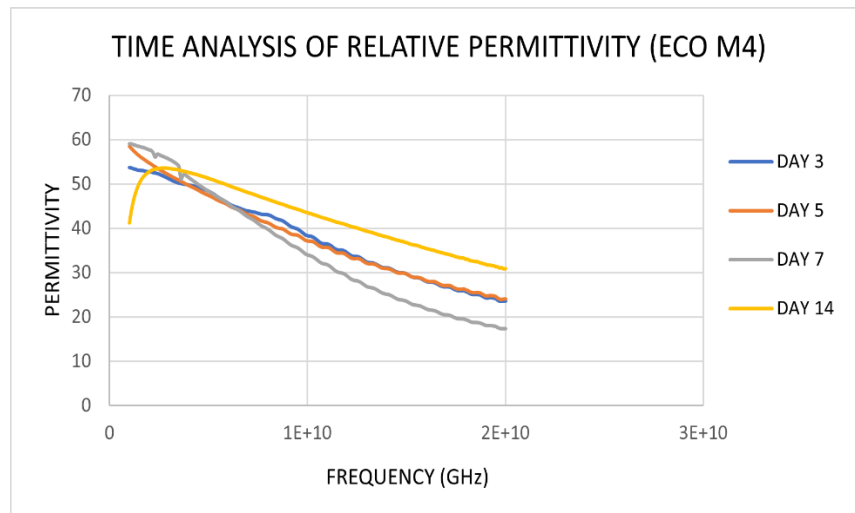
Figure 4.28: Time analysis of relative permittivity of ECO M4

The ECO M4 muscle phantom shows the most consistent graph trend, where on day three and day 5, the fluctuation on the graph can be seen as almost similar with a slight difference. On day seven, the graph trends show the relative permittivity value increases and decreases proportionally. On day 14, the graph shows a drastic decrease in the graph trend where the huge gap was observed, inverse proportionally to the previous trend. The muscle phantom can be considered relevant compared with human skin tissue.
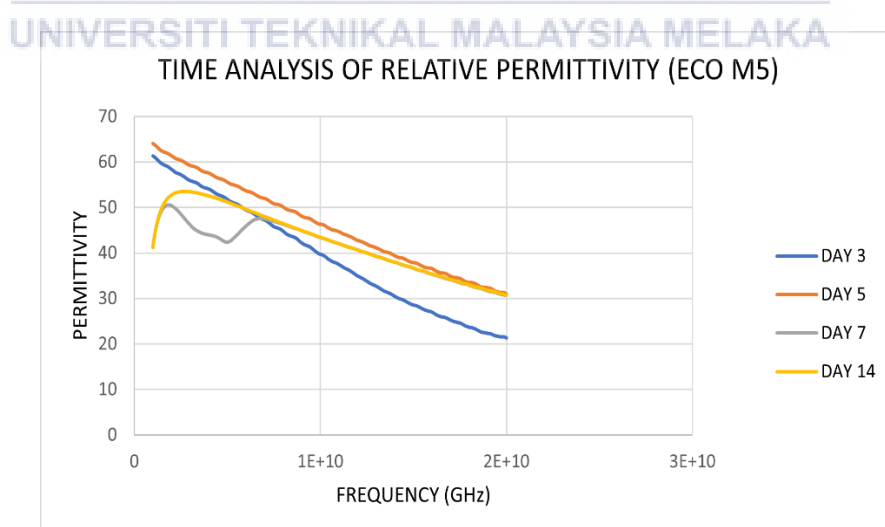
Figure 4.29: Time analysis of relative permittivity of ECO M5

The ECO M5 skin phantom is also one of 5 muscle tissue phantoms that consistently shows a promising trend after M4 to keep the trends directly proportional. However, after seven days of preservation, the graph started to show the unreasonable shape of the trend, wherein in the low-frequency range, the fluctuation is noticeable and only consistent in the middle range frequency; after 14 days, the graph started to show an inversely proportional to the usual trend where does no longer compatible on the low-frequency range.

4.3.5 The analysis of loss tangent of muscle tissue phantom in 14 days.
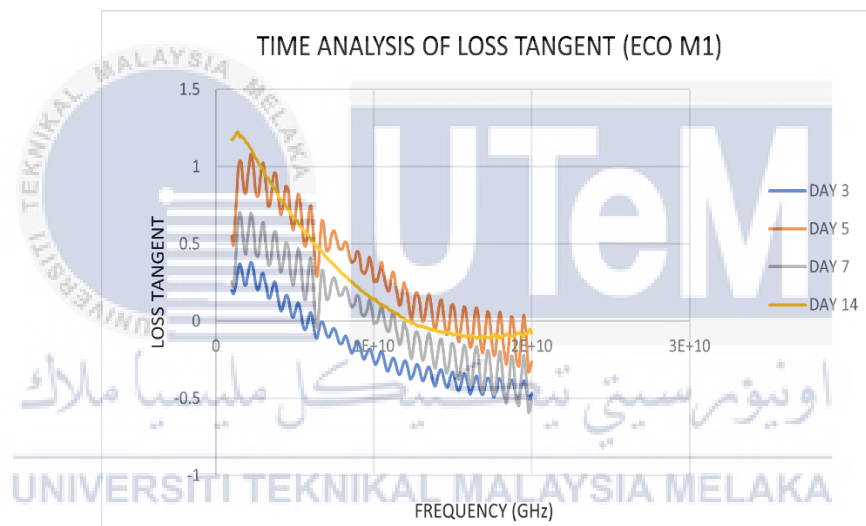
Figure 4.30: Time analysis of loss tangent of ECO M1
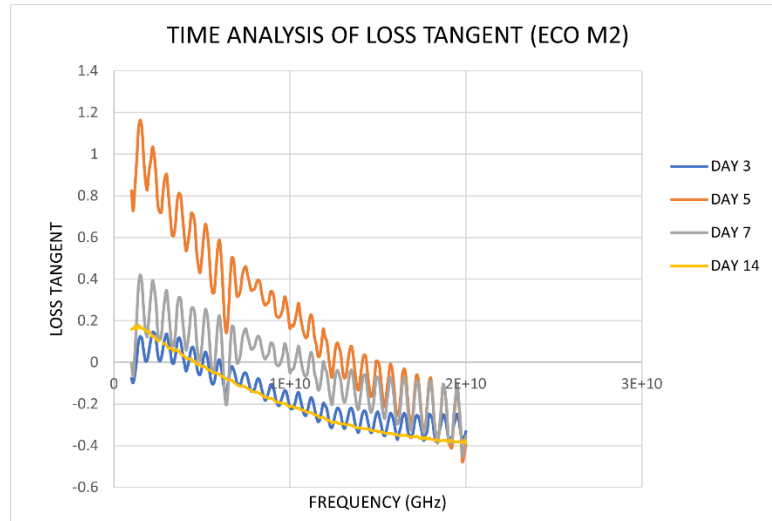
Figure 4.31: Time analysis of loss tangent of ECO M2
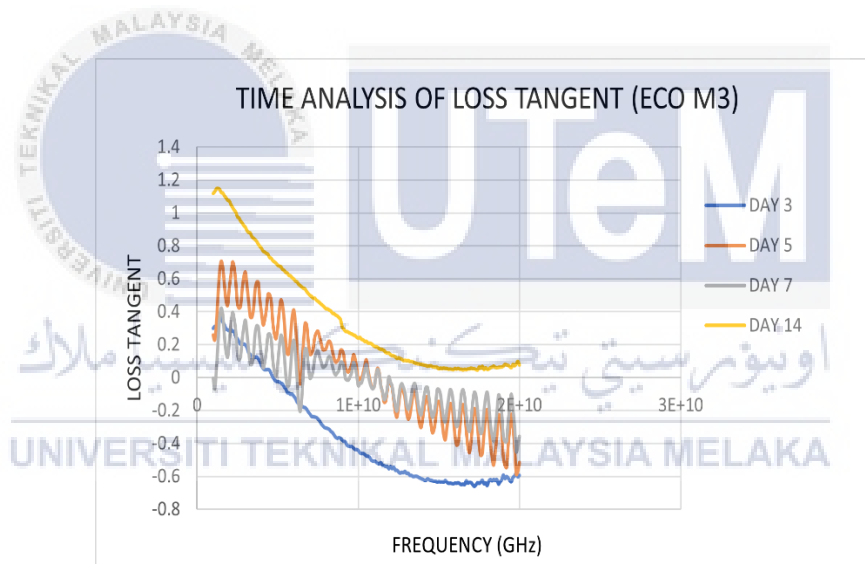
Figure 4.32: Time analysis of loss tangent of ECO M3
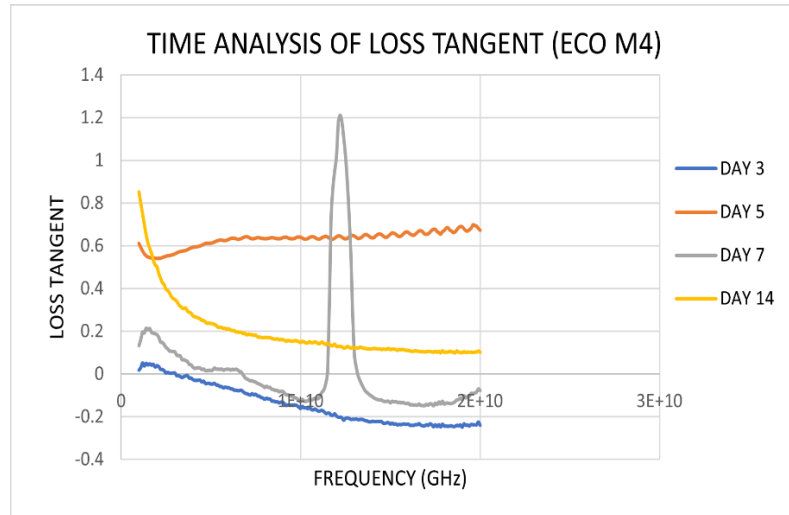
Figure 4.33: Time analysis of loss tangent of ECO M4
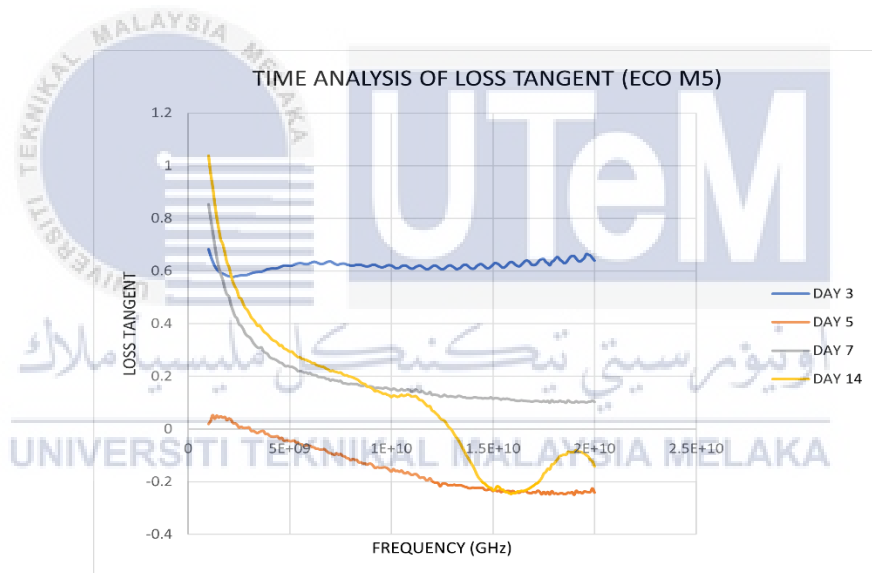
Figure 4.34: Time analysis of loss tangent of ECO M5

4.4 Comparison of relative permittivity with recent papers

4.4.1 Comparison of relative permittivity of skin tissue phantom
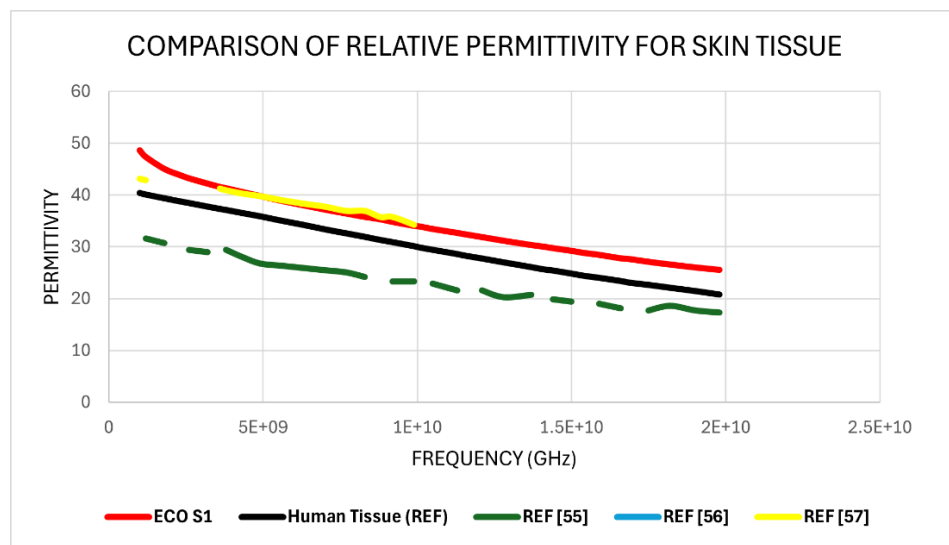
Figure 4.35: Comparison of relative permittivity with recent papers [55], [56], and [57]

The graph above and the statistics from the present article show that eco-friendly-based materials for skin tissue phantoms are comparable to human skin tissue. With modest adjustments in the graph trend, the eco-friendly materials are on par with the non-eco-friendly tissue phantom.

A comparison of relative permittivity with respect to frequency was performed using the (ECO S1) skin phantom and the recent journal studies [55], [56], and [57]. All of the data indicates a similar trend to genuine human skin. However, the relative permittivity of REF [55] is relatively low at low frequencies and quite close to human skin at high frequencies. REF [56] and REF [57] are nearly identical to human skin, but REF [56] only goes up to 10 GHz. (ECO S1) approximates ideal relative permittivity to human skin. In conclusion, (ECO S1) is capable of simulating the relative permittivity to human skin when compared to other results from recent articles the most.

4.4.2   Comparison of relative permittivity of fat tissue phantom
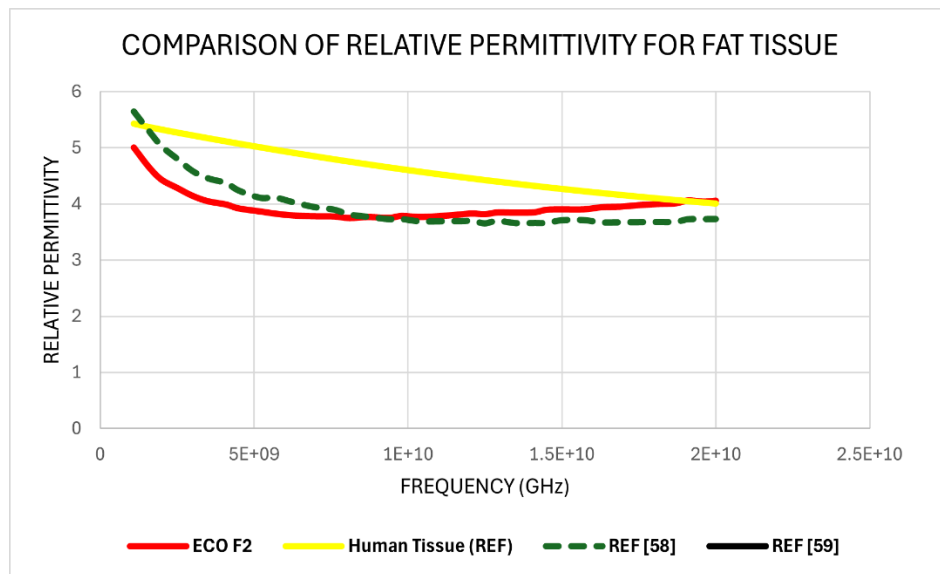
Figure 4.36: Comparison of relative permittivity of ECO fat tissue 2, human tissue, [58] and [59]

The graph above and the information from the data supplied in the current journal demonstrate that eco-friendly-based materials for fat tissue phantoms are comparable to human fat tissue. The eco-friendly elements are on par with the non-eco-friendly tissue phantom, with minor changes in the graph trend.

The graph compares the relative permittivity value of fat samples to recent articles shows that, the fat phantom (ECO f2) and REF [59] are almost identical to human fat, while REF [58] is almost identical at low and high frequency. When compared to human fat, the relative permittivity of fat phantom (ECO f2) and REF [58] shows good agreement.

4.4.3   Comparison of relative permittivity of muscle phantom
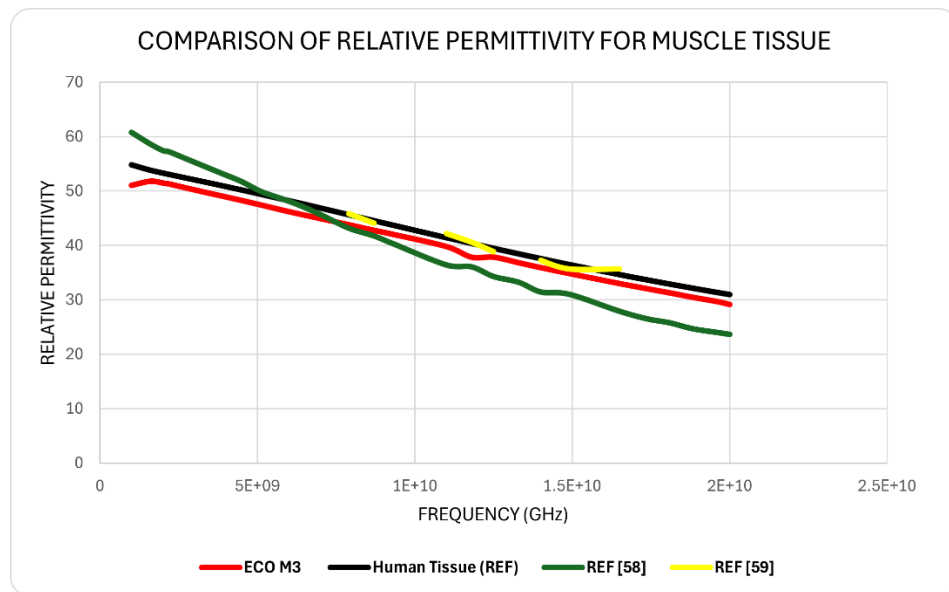
Figure 4.37: Comparison of relative permittivity of ECO muscle tissue 3, human tissue, [58] and [59]

The graph above, combined with the knowledge gathered from the data provided in the current journal, shows that eco-friendly-based materials for muscle tissue phantoms are comparable to human fat tissue. The eco-friendly elements are on par with the non-eco-friendly tissue phantom; the developed muscle tissue can mimic the human tissue phantom the most.

The graph compares the relative permittivity value of muscle samples to recent articles. REF [58] exhibits excellent relative permittivity across the whole frequency band. REF [59] indicates a perfect match to human muscle tissue in the frequency range of 5-7 GHz, while SAMPLE 3 demonstrates a perfect match to human muscle tissue in the frequency range of 15-20 GHz. Finally, REF [59] has the highest similarity to human muscle tissue.

4.5 **Tissue equivalent phantom validation by using the split ring resonator sensor.**

Validation is critical in research because it verifies the accuracy and quality of the acquired data before it is processed and analysed. Furthermore, in qualitative research, validation boosts confidence in the findings and gives the best support for making financial decisions.

The purpose of the tissue-equivalent phantom tissue was to mimic human tissue's radiological and physical characteristics. These phantoms replicate the human body for testing and calibration in medical research for medical devices, imaging, and therapy. For example, the tissue equivalent phantom was used for the on or in-body antenna or antenna implant testing. It is used in developing and testing novel medical techniques and assessing the effectiveness of medical imaging apparatuses. The validation of the tissue equivalent phantoms will help to ensure the characterization of the most suitable materials to be used in certain conditions or circumstances depending on the medical research needs.

4.5.1 **Validate with split ring resonator sensor.**
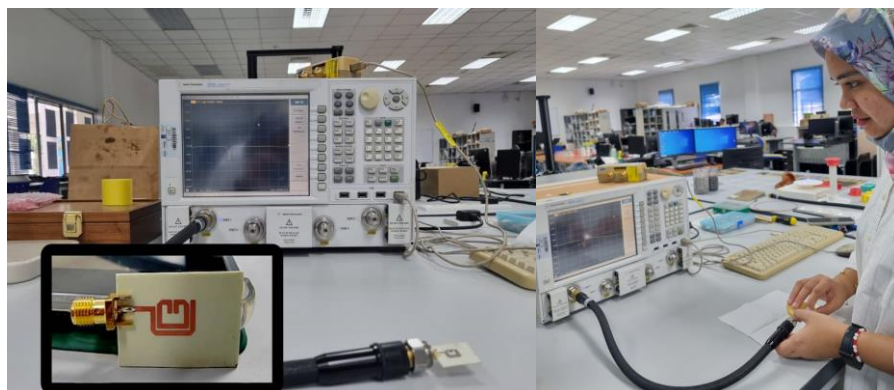
Figure 4.38: Tissue phantom testing on split ring resonator using VNA.

A split-ring resonator (SRR) sensor is a type of electromagnetic sensor that detects changes in the surrounding electromagnetic environment by utilizing the features of split-ring resonators. When exposed to an electromagnetic field, the resonator can resonate at a specified frequency. Any changes in the surrounding environment, such as temperature, pressure, or the presence of particular materials, might impact the split-ring resonator's resonance frequency. This SRR runs at 2.8-3.8GHz and can be used to detect varied degrees of moisture. Shifting resonant peaks detect the dielectric property of the material [51] [52].

A Vector Network Analyzer (VNA) can measure the resonant frequency of a split-ring resonator (SRR). Set up the VNA to measure the SRR's resonance frequency. Connect the SRR to the VNA ports and record the S21 parameter (forward/reverse power ratio) as a function of frequency [60]. Consider parameters such as dielectric constant, loss tangent, and material thickness while selecting materials for the SRR [61].

A Vector Network Analyzer (VNA) must first be calibrated before measuring the resonant frequency of a split-ring resonator (SRR). Before measuring, the probe must also be calibrated. After that, the SRR is linked to the VNA ports, and the VNA is configured to measure the S21 parameter as a function of frequency. The measured S21 parameter data is then analysed to identify the SRR's resonant frequency, which may then be compared to estimated and simulated values to validate the SRR's design and performance.

4.5.2 The validation process → skin, fat, and muscle phantom
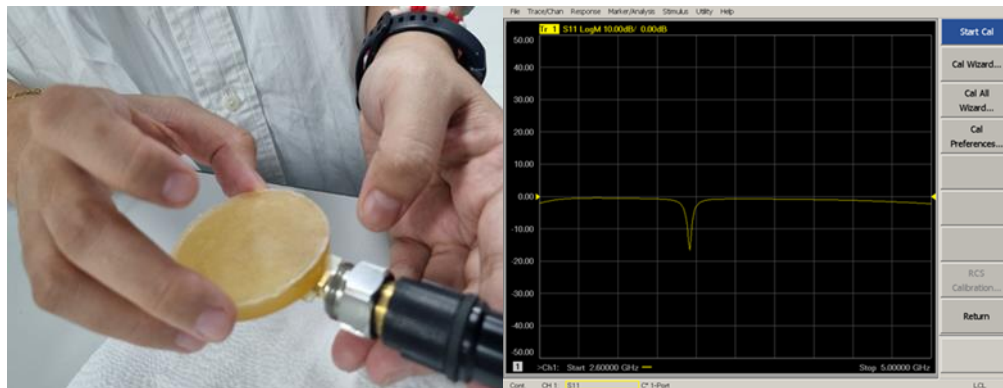
Figure 4.39: Skin tissue phantom validation

Figure 4.39 shows the display on the vector network analyzer shifts due to the high permittivity of skin tissue; the narrow shifting reveals the high permittivity of the skin phantom. This problem is addressed by the split resonator ring approach, which yields precise permittivity values for skin tissue phantoms. This method has been applied in several investigations, such as the utilization of nine-antenna sensor arrays inspired by metamaterials for breast phantom imaging [62].
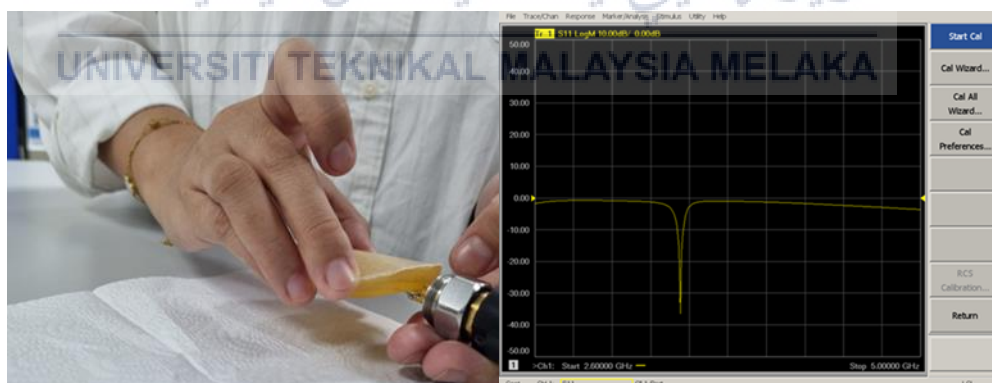
Figure 4.40: Fat tissue phantom validation

Figure 4.40 shows the split resonator ring is used to assess the permittivity of complex materials, such as biological tissues [63]. The shift in resonance frequency is proportional to the sample's permittivity, allowing for precise measurements of the

sample's complex permittivity. The low permittivity of fat tissue causes the vector network analyzer display to change. It accurately measures the permittivity of fat tissue phantoms where the fat content is the lowest.
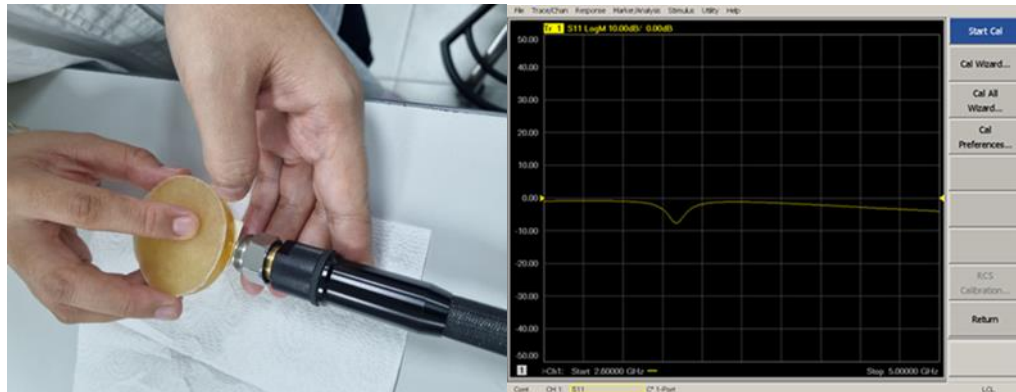
Figure 4.41: Muscle tissue phantom validation

The figure 4.41 shows the split ring resonator is used as microwave resonator that generates a non-uniform field that can detect variations in frequency response induced by changes in the permittivity of the muscle [64]. It measures its ability to store electrical energy in an electric field. For muscle tissue validation, split ring resonators (SRR) coupled to a vector network analyzer are utilized, and SRRs are used to assess muscle quality and differentiate between skin tissue phantom and fat tissue phantom. The muscle displays the less narrow band with the maximum permittivity.

Table 4.10: Table of relative permittivity with respect to frequency (GHz) and magnitude (dB)

Tissue	Permittivity	Frequency (GHz)	Magnitude (dB)
Reference	1	3.7	-
Skin	37.092	3.40	-15.54
Fat	5.1739	3.52	-128.4
Muscle	51.44	3.52	4.81dB

CHAPTER 5

CONCLUSION AND FUTURE WORKS
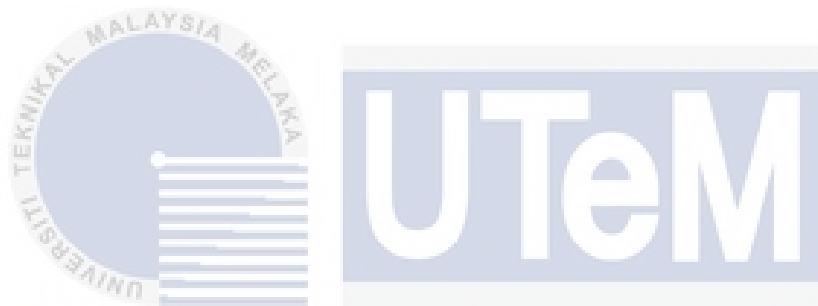
5.1 Conclusion

Animal testing has been a common practice in biomedical engineering for decades. However, the use of animals in research has been a topic of debate due to ethical concerns and the potential harm caused to animals. To address this issue, researchers have been exploring using tissue-equivalent phantoms as an alternative to animal testing. These phantoms are designed to mimic human tissues' physical and chemical properties, making them ideal for testing the safety and efficacy of medical devices and cosmetics. Researchers can re-evaluate the number of animal tests done throughout the years using these phantoms. This approach reduces the number of animals used in research and provides more accurate results, as the phantoms are designed to mimic human tissues. Developing tissue-equivalent phantoms is an

essential step towards reducing the use of animals in research and ensuring the safety of medical devices and cosmetics.

This thesis discusses the comprehensive characterization and analysis of eco-friendly ingredients in tissue-equivalent phantom development for biomedical microwave applications. Three types of phantoms can be mimicked and have been developed by previous researchers: solid, liquid, and semi-solid. In this project, the focus was on semi-solid types of phantoms because they are very close to human tissue structure, and they are the best for developing skin, fat, and muscle tissue phantoms. Comprehensive characterization and analysis of eco-friendly ingredients in tissue-equivalent phantom development for biomedical microwave application have been done correctly to ensure the best ingredients used to develop the tissue phantom have a unique characteristic. They function as an application for every phantom grown. The most important thing is to choose bio-compatible and eco-friendly ingredients.

The fabrication process involved measuring every ingredient used based on the recipe obtained from the previous paper. Two types of cooking methods are used to develop the tissue phantom: direct heating and double boiling. In direct heating, the mixture is directly exposed to a heat source on an open flame, which is the induction cooker, and this method has the heat applied directly to the mix, causing it to cook or heat up evenly. Besides double Boiling, Double boiling is a cooking technique where the mixture is placed in a container or beaker and then inside a larger pot filled with water. The water in the outer pot is heated, and the steam generated gently cooks the food in the inner pot.

All the tissue phantoms were measured within the frequency range of 1GHz-20GHz using the Agilent Technologies 85070E dielectric probe kit paired with an

Agilent Technologies N5242A Network Analyzer. Hence, these phantom developments aim not only to use eco-friendly and bio-compatible ingredients but also to be measured across 1GHz-20GHz. These phantoms were then measured and analysed based on the dielectric properties, relative permittivity, and loss tangent. From the analysis obtained, most of the samples show almost the same trend as human tissue, and one of the tissues shows a nearly perfect trend to human tissue references, compared with the recent journal.

Moreover, each eco-friendly tissue phantom, skin fat and muscle were measured on different days to analyse the stability of the dielectric properties within 14 days. Some samples show consistency in the dielectric properties, and some do not; this may be due to the difference in the ingredients that affect the durability of the phantom. As the defence, this may also be due to the ecofriendly-based ingredients-based phantom and the unavailability of the preservatives such as PEP are used to ensure the tissue phantom can last longer compared to the ecofriendly-based tissue phantom.

Last but not least, this project best believe has contributed to the sustainable development impact in society, especially in terms of the environment where the numbers of animal testing have been reduced, and the ethical standards in science and industry have been by promoting a more compassionate and sustainable approach to research and development. Overall, reducing animal killing for testing can benefit the environment by promoting conservation and reducing carbon emissions and pollution. Furthermore, above all of this, the use of eco-friendly and biocompatible ingredients in tissue phantom development helps to achieve sustainable development goal number three: GOOD HEALTH and WELL-BEING, where it can be applied in research in

medicine to test brand new medication and medical procedures to examine the consequences of the diseases by replacing the animal testing.

5.2   Future works

Tissue phantom development is an essential tool in biomedical engineering for testing, calibrating, and validating, especially in biomedical engineering. Tissue-equivalent phantoms are usually used to stimulate the properties of human tissue in medical imaging, new devices, and drug testing. Tissue phantoms are designed to mimic composition and radiation attenuation. These phantoms are used to calibrate and test medical imaging equipment and evaluate the accuracy of the devices and the drugs as treatment plans. Developing tissue-equivalent phantoms using biocompatible and eco-friendly ingredients can be very challenging, especially in ensuring their ability to function as the phantoms that are made using active and harmful chemicals that are more potent because the aims are to provide these materials should mimic human tissue properties in terms of mechanical properties, optical, relative permittivity and also loss tangent.

With the rapid development of medical devices and new imaging modalities, such as photoacoustic imaging and terahertz imaging, there is a need for tissue-equivalent phantom that can stimulate the properties of biological tissues at these frequencies. Several things could be improved during this project's development and measuring process. One of them is the limitation in the frequency used. The Vector Network analyzer (VNA) in the MRG lab is operated at 24GHz only when many applications can be made with a higher frequency range, especially for biomedical purposes.

Besides, nowadays, there is still no phantom simultaneous PET/MRI acquisition which combines the functional information of PET with high resolution in anatomical images of MRI. Therefore, there is a need for tissue phantom equivalent to address these issues since finding suitable materials that can match the exact match to optical, mechanical, and dielectric properties of different types of tissues, especially to apply it in the frequently high frequency properties, may vary depending on the wavelength, frequency, or the modality of the treatment plan.

Based on the results obtained from this research, a multi-layer skin, fat, and muscle can be used to develop arm or leg phantom for testing purposes. Not only limited to that, but specific organs can also be mimicked using the same properties found throughout the research, such as kidneys, lungs, and breast phantom. This future work can be applied for testing the implanted device, such as a graphene-based antenna, to study its function because it has the structure of the phantom, mimicking the real human organ, and it can be beneficial for medical student study purposes.

Moreover, in the near future, the development of new materials that can more accurately simulate the properties of biological tissues by exploring the use of new materials and fabrication techniques to create phantoms with more realistic tissue properties and accurately mimic all the dielectric properties of human tissues and it can be used to validate the performance of medical imaging system. Future research can focus on developing a more suitable tissue equivalent phantom that can be used to test and optimize radiation therapy systems. Future research can explore the use of phantoms in other areas of therapy, such as ultrasound therapy and magnetic resonance imaging, and tailor them to specific applications, such as tumour detection on the breast and brain.

REFERENCES

[1] M. Z. Vardaki and N. Kourkoumelis, "Tissue Phantoms for Biomedical Applications in Raman Spectroscopy: A Review," *https://doi.org/10.1177/1179597220948100*, vol. 11, p. 117959722094810, Aug. 2020, doi: 10.1177/1179597220948100.

[2] A. T. Mobashsher and A. M. Abbosh, "Artificial human phantoms: Human proxy in testing microwave apparatuses that have electromagnetic interaction with the human body," *IEEE Microw. Mag.*, vol. 16, no. 6, pp. 42–62, 2015, doi: 10.1109/MMM.2015.2419772.

[3] "Medical gallery of Blausen Medical 2014," *WikiJournal Med.*, vol. 1, no. 2, 2014, doi: 10.15347/WJM/2014.010.

[4] M. S. Islam, M. T. Islam, and A. F. Almutairi, "Experimental tissue mimicking human head phantom for estimation of stroke using IC-CF-DMAS algorithm in microwave based imaging system," *Sci. Reports 2021 111*, vol. 11, no. 1, pp. 1–14, Nov. 2021, doi: 10.1038/s41598-021-01486-x.

[5] J. S. T. Thilagam, D. M. V. R. Vittal, D. G. A. Khan, and B. S. Reddy,

"Measurement and Analysis of Vector Network Analyzer," *Int. J. Eng. Adv. Technol.*, vol. 11, no. 6, pp. 41–46, Aug. 2022, doi: 10.35940/IJEAT.F3681.0811622.

[6]   Maciej Serda *et al.*, "Synteza i aktywność biologiczna nowych analogów tiosemikarbazonowych chelatorów żelaza," *Uniw. śląski*, vol. 7, no. 1, pp. 343–354, 2013, doi: 10.2/JQUERY.MIN.JS.

[7]   D. M. Peterson *et al.*, "A tissue equivalent phantom of the human torso for in vivo biocompatible communications," *IFMBE Proc.*, vol. 32 IFMBE, pp. 414–417, 2010, doi: 10.1007/978-3-642-14998-6_105.

[8]   N. A. Kabir, F. O. Okoh, and M. F. Mohd Yusof, "Radiological and physical properties of tissue equivalent mammography phantom: Characterization and analysis methods," *Radiat. Phys. Chem.*, vol. 180, no. October 2020, p. 109271, 2021, doi: 10.1016/j.radphyschem.2020.109271.

[9]   H. Cook *et al.*, "Development of optimised tissue-equivalent materials for proton therapy," *Phys. Med. Biol.*, vol. 68, no. 7, 2023, doi: 10.1088/1361-6560/acb637.

[10]   A. Mirbeik and N. Ebadi, "Deep learning for tumor margin identification in electromagnetic imaging," *Sci. Rep.*, vol. 13, no. 1, pp. 1–11, 2023, doi: 10.1038/s41598-023-42625-w.

[11]   A. P. Gregory, K. Quéléver, D. Allal, and O. Jawad, "Validation of a broadband tissue-equivalent liquid for sar measurement and monitoring of its dielectric properties for use in a sealed phantom," *Sensors (Switzerland)*, vol. 20, no. 10,

2020, doi: 10.3390/s20102956.

[12] "Magnetic Resonance in Med - 2017 - Ianniello - Synthesized tissue-equivalent dielectric phantoms using salt and.pdf." .

[13] C. K. McGarry *et al.*, "Tissue mimicking materials for imaging and therapy phantoms: a review," *Phys. Med. Biol.*, vol. 65, no. 23, p. 23TR01, Dec. 2020, doi: 10.1088/1361-6560/ABBD17.

[14] A. Turgut and B. K. Engiz, "Analyzing the SAR in Human Head Tissues under Different Exposure Scenarios," *Appl. Sci.*, vol. 13, no. 12, 2023, doi: 10.3390/app13126971.

[15] L. Farina, K. Sumser, G. van Rhoon, and S. Curto, "Thermal characterization of phantoms used for quality assurance of deep hyperthermia systems," *Sensors (Switzerland)*, vol. 20, no. 16, pp. 1–9, 2020, doi: 10.3390/s20164549.

[16] M. Z. Vardaki and N. Kourkoumelis, "Tissue Phantoms for Biomedical Applications in Raman Spectroscopy: A Review," *Biomed. Eng. Comput. Biol.*, vol. 11, p. 117959722094810, 2020, doi: 10.1177/1179597220948100.

[17] L. Ntombela, B. Adeleye, and N. Chetty, "Low-cost fabrication of optical tissue phantoms for use in biomedical imaging," *Heliyon*, vol. 6, no. 3, p. e03602, Mar. 2020, doi: 10.1016/J.HELIYON.2020.E03602.

[18] C. -K Chou, G. -W Chen, A. W. Guy, and K. H. Luk, "Formulas for preparing phantom muscle tissue at various radiofrequencies," *Bioelectromagnetics*, vol. 5, no. 4, pp. 435–441, 1984, doi: 10.1002/BEM.2250050408.

[19] S. Jenne and H. Zappe, "Multiwavelength tissue-mimicking phantoms with tunable vessel pulsation," *J. Biomed. Opt.*, vol. 28, no. 04, pp. 1–13, 2023, doi: 10.1117/1.jbo.28.4.045003.

[20] S. Wilby, A. Palmer, W. Polak, and A. Bucchi, "A review of brachytherapy physical phantoms developed over the last 20 years: Clinical purpose and future requirements," *Journal of Contemporary Brachytherapy*, vol. 13, no. 1. Termedia Publishing House Ltd., pp. 101–115, 2021, doi: 10.5114/JCB.2021.103593.

[21] R. Prakash, K. K. Yamamoto, S. R. Oca, W. Ross, and P. J. Codd, "Brain-Mimicking Phantom for Photoablation and Visualization," ... *Int. Symp. Med. Robot. Int. Symp. Med. Robot.*, vol. 2023, 2023, doi: 10.1109/ISMR57123.2023.10130243.

[22] S. Di Meo, G. Matrone, and M. Pasian, "Experimental Validation on Tissue-Mimicking Phantoms of Millimeter-Wave Imaging for Breast Cancer Detection," *Appl. Sci. 2021, Vol. 11, Page 432*, vol. 11, no. 1, p. 432, Jan. 2021, doi: 10.3390/APP11010432.

[23] A. Hossain *et al.*, "Sensor-based microwave brain imaging system (SMBIS): An experimental six-layered tissue based human head phantom model for brain tumor diagnosis using electromagnetic signals," *Eng. Sci. Technol. an Int. J.*, vol. 45, no. August, p. 101491, 2023, doi: 10.1016/j.jestch.2023.101491.

[24] G. Anand and A. Lowe, "Investigating electrical impedance spectroscopy for estimating blood flow-induced variations in human forearm," *Sensors (Switzerland)*, vol. 20, no. 18, pp. 1–14, 2020, doi: 10.3390/s20185333.

[25]   H. Dobšíček Trefná, S. Llacer Navarro, F. Lorentzon, T. Nypelö, and A. Ström, "Fat tissue equivalent phantoms for microwave applications by reinforcing gelatin with nanocellulose," *Biomed. Phys. Eng. express*, vol. 7, no. 6, Nov. 2021, doi: 10.1088/2057-1976/AC2634.

[26]   J. Liu, Ö. Atmaca, and P. P. Pott, "Needle-Based Electrical Impedance Imaging Technology for Needle Navigation," *Bioengineering*, vol. 10, no. 5, pp. 1–14, 2023, doi: 10.3390/bioengineering10050590.

[27]   S. Di Meo *et al.*, "Tissue-mimicking materials for breast phantoms up to 50 GHz," *Phys. Med. Biol.*, vol. 64, no. 5, p. 055006, Feb. 2019, doi: 10.1088/1361-6560/AAFEEC.

[28]   N. Nakanishi *et al.*, "Rectus Femoris Mimicking Ultrasound Phantom for Muscle Mass Assessment: Design, Research, and Training Application," *J. Clin. Med.*, vol. 10, no. 12, p. 2721, Jun. 2021, doi: 10.3390/JCM10122721.

[29]   N. Yadav, M. Singh, and S. P. Mishra, "Tissue-equivalent materials used to develop phantoms in radiation dosimetry: A review," *Mater. Today Proc.*, vol. 47, pp. 7170–7173, Jan. 2021, doi: 10.1016/J.MATPR.2021.06.359.

[30]   B. McDermott *et al.*, "Stable tissue-mimicking materials and an anatomically realistic, adjustable head phantom for electrical impedance tomography," *Biomed. Phys. Eng. Express*, vol. 4, no. 1, Jan. 2018, doi: 10.1088/2057-1976/AA922D.

[31]   W. E. Morton and J. W. S. Hearle, "Physical Properties of Textile Fibres: Fourth Edition," *Phys. Prop. Text. Fibres Fourth Ed.*, pp. 1–776, 2008, doi:

10.1533/9781845694425.

[32] M. Sergolle, X. Castel, M. Himdi, P. Besnier, and P. Parneix, "Structural composite laminate materials with low dielectric loss: Theoretical model towards dielectric characterization," *Compos. Part C Open Access*, vol. 3, no. June, pp. 1–8, 2020, doi: 10.1016/j.jcomc.2020.100050.

[33] "Dielectric Properties of Body Tissues: HTML clients." http://niremf.ifac.cnr.it/tissprop/htmlclie/htmlclie.php (accessed Jan. 10, 2024).

[34] C. Gabriel, S. Gabriel, and E. Corthout, "The dielectric properties of biological tissues: I. Literature survey," *Phys. Med. Biol.*, vol. 41, no. 11, pp. 2231–2249, 1996, doi: 10.1088/0031-9155/41/11/001.

[35] S. Gabriel, R. W. Lau, and C. Gabriel, "The dielectric properties of biological tissues: III. Parametric models for the dielectric spectrum of tissues," *Phys. Med. Biol.*, vol. 41, no. 11, pp. 2271–2293, 1996, doi: 10.1088/0031-9155/41/11/003.

[36] M. M. Nguyen, S. Zhou, J. luc Robert, V. Shamdasani, and H. Xie, "Development of oil-in-gelatin phantoms for viscoelasticity measurement in ultrasound shear wave elastography," *Ultrasound Med. Biol.*, vol. 40, no. 1, pp. 168–176, 2014, doi: 10.1016/j.ultrasmedbio.2013.08.020.

[37] C. Fontes-Candia *et al.*, "Maximizing the oil content in polysaccharide-based emulsion gels for the development of tissue mimicking phantoms," *Carbohydr. Polym.*, vol. 256, no. December 2020, 2021, doi: 10.1016/j.carbpol.2020.117496.

[38]   L. A. MacQueen *et al.*, "Muscle tissue engineering in fibrous gelatin: implications for meat analogs," *npj Sci. Food*, vol. 3, no. 1, pp. 1–12, 2019, doi: 10.1038/s41538-019-0054-8.

[39]   L. C. Cabrelli, P. I. B. G. B. Pelissari, A. M. Deana, A. A. O. Carneiro, and T. Z. Pavan, "Stable phantom materials for ultrasound and optical imaging," *Phys. Med. Biol.*, vol. 62, no. 2, pp. 432–447, 2017, doi: 10.1088/1361-6560/62/2/432.

[40]   A. Arya, M. Sadiq, and A. L. Sharma, "Salt concentration and temperature dependent dielectric properties of blend solid polymer electrolyte complexed with NaPF6," *Mater. Today Proc.*, vol. 12, no. May, pp. 554–564, 2019, doi: 10.1016/j.matpr.2019.03.098.

[41]   J. Linford, S. Shalev, J. Bews, R. Brown, and H. Schipper, "Development of a tissue equivalent phantom for diaphanography," *Med. Phys.*, vol. 13, no. 6, pp. 869–875, 1986, doi: 10.1118/1.595948.

[42]   D. W. Hanzon, K. Yu, and C. M. Yakacki, *Activation Mechanisms of Shape-Memory Polymers*. Elsevier Inc., 2017.

[43]   R. A. K. Possomato-Vieira, José S. and Khalil and O. 2. 0. E. S. E. and S. Modeling, "乳鼠心肌提取 HHS Public Access," *Physiol. Behav.*, vol. 176, no. 12, pp. 139–148, 2017, doi: 10.3109/02656736.2016.1145745.Thermochromic.

[44]   T. Slanina, D. H. Nguyen, J. Moll, and V. Krozer, "Temperature dependence studies of tissue-mimicking phantoms for ultra-wideband microwave breast tumor detection," *Biomed. Phys. Eng. Express*, vol. 8, no. 5, 2022, doi:

10.1088/2057-1976/ac811b.

[45] T. Le, H. Tran, B. Pejcinovic, K. G. R. Thompson, R. Doneker, and A. Ramachandran, "Development and Characterization of Carbon-Fiber Based Magnetically Loaded Microwave Absorber Material," *IEEE Int. Symp. Electromagn. Compat.*, vol. 2018-Augus, pp. 767–771, 2018, doi: 10.1109/EMCEurope.2018.8485065.

[46] S. Guide, "Keysight Technologies PNA and ENA Network Analyzers Frequency Converter and Mixer Test."

[47] K. Y. You, "Introductory Chapter: RF/Microwave Applications," *Emerg. Microw. Technol. Ind. Agric. Med. Food Process.*, no. July, 2018, doi: 10.5772/intechopen.73574.

[48] Keysight Techonologies, "Keysight 85070E Dielectric Probe Kit 200 MHz to 50 GHz Technical Overview," 2017.

[49] A. La Gioia, E. Porter, I. Merunka, A. Shahzad, S. Salahuddin, and M. Jones, "diagnostics Open-Ended Coaxial Probe Technique for Dielectric Measurement of Biological Tissues: Challenges and Common Practices," doi: 10.3390/diagnostics8020040.

[50] G. Brodie, M. V. Jacob, and P. Farrell, "6 Techniques for Measuring Dielectric Properties," *Microw. Radio-Frequency Technol. Agric.*, pp. 52–77, 2015, doi: 10.1515/9783110455403-007.

[51] J. J. L. Morton and J. J. L. Morton, "Electrical and optical properties of materials Part 1 . Conductivity : from insulators to su- perconductors," vol. 0,

pp. 1–29.

[52] Ł. J. Walczak-Nowicka and M. Herbet, "Sodium Benzoate—Harmfulness and Potential Use in Therapies for Disorders Related to the Nervous System: A Review," *Nutrients*, vol. 14, no. 7, 2022, doi: 10.3390/nu14071497.

[53] E. M. Ahmed, "Hydrogel: Preparation, characterization, and applications: A review," *J. Adv. Res.*, vol. 6, no. 2, pp. 105–121, 2015, doi: 10.1016/j.jare.2013.07.006.

[54] Z. Chen, "A Microwave Sensor for Leaf Moisture Detection Based on Split-Ring Resonator," vol. 00, pp. 2020–2022, 2020.

[55] "Electronics Letters - 2014 - Aminzadeh - Theoretical and experimental broadband tissue-equivalent phantoms at microwave and.pdf." .

[56] S. Paul, *Biomedical engineering and its applications in healthcare*. 2019.

[57] A. E. Forte, S. Galvan, F. Manieri, F. Rodriguez y Baena, and D. Dini, "A composite hydrogel for brain tissue phantoms," *Mater. Des.*, vol. 112, pp. 227–238, 2016, doi: 10.1016/j.matdes.2016.09.063.

[58] L. Joseph, "Examensarbete 30 hp Development of Ultra-Wide band 500 MHz-20 GHz Heterogeneous Multi-Layered Phantom Comprising of Human Skin, Fat and Muscle Tissues for Various Microwaves Based Biomedical Applications," no. December, 2018, [Online]. Available: http://www.teknat.uu.se/student.

[59] T. Yilmaz, R. Foster, and Y. Hao, "Broadband tissue mimicking phantoms and

a patch resonator for evaluating noninvasive monitoring of blood glucose levels," *IEEE Trans. Antennas Propag.*, vol. 62, no. 6, pp. 3064–3075, 2014, doi: 10.1109/TAP.2014.2313139.

[60] J. Chilo Supervisor and K. Prytz, "Design of Singly Split Single Ring Resonator for Measurement of Dielectric Constant of Materials using Resonant Method Master's Program in Electronics/Telecommunications," no. June, 2013.

[61] R. Mustafa, "Ring Resonator with single gap for Measurement of Dielectric Constants of Materials," *Univ. Gavle*, no. June, pp. 1–40, 2013.

[62] M. T. Islam, M. Samsuzzaman, M. T. Islam, and S. Kibria, "Experimental breast phantom imaging with metamaterial-inspired nine-antenna sensor array," *Sensors (Switzerland)*, vol. 18, no. 12, 2018, doi: 10.3390/s18124427.

[63] M. Alibakhshikenari *et al.*, "Design of a Planar Sensor Based on Split-Ring Resonators for Non-Invasive Permittivity Measurement," *Sensors*, vol. 23, no. 11, 2023, doi: 10.3390/s23115306.

[64] V. Mattsson *et al.*, "Mas: Standalone microwave resonator to assess muscle quality," *Sensors*, vol. 21, no. 16, 2021, doi: 10.3390/s21165485.

APPENDICES

.

Guar Gum

Specification

Moisture %	9.33
Ash%	0.73
Protein%	4.02
ACID INSOLUBLE MATTER%	2.54
Glactomannan %	83.38
Ph	6.42
PHYSICAL ANALYSIS	
Appearance	Light Cream Coloured homogeneous Powder
Granulometry	NIL
On 100 mesh %	
Through 200 mesh %	98.35
VISCOSITY (Brookfield)	
2 Hours	5100
24 Hours	5200
MICROBIOLGICAL ANALYSIS	
Total Plate Count (cfu/g)	1200
Yeast & Molds (cfu/g)	10
Ecoli (cfu/g)	Absent
Salmonella (cfu/25g)	Absent
Starch	Absent
HEAVY METALS	
Arsenic	< 1 ppm
Lead	< 1 ppm
Mercury	ND
Cadmium	ND
Heavy Metals (As Pb) pm	< 2 ppm

Material has been passed from Metal detector
BROOKFIELD VISCOSITY- Viscosity is measured at 1% solution , on Brookfield
Viscometer RVT model using spindle no. 4 at 20 RPM, Temperature at@25°C.

APPENDIX A: Spec-Guar Gum

Maltodextrin

Specification

Parameters	Specification
Appearance	White powder and no fixed shape
Smell	Has special smell of maltodextrin and no exceptional smell
Taste	Sweetness or slightly sweetness, no other taste
DE%(m/m)	10-12
Starch Test	Negative
Moisture%(m/m)	≤6.0
Solubility%(m/m)	≥98
pH	4.6 – 6.5
Ash%(m/m)	<0.6
Iodine experiment	No blue reaction

Heavy Metal Analysis

As mg/kg	≤1.0
Pb mg/kg	≤0.5
Sulfur Dioxide g/kg	≤0.04

Microbiological Analysis

Total Plate Count	≤3000
Colinforms MPN/100g	≤30
Pathogenic Bacterium	No exist

Appendix B: Spec- Maltodextrin

Eva Chem

NAME OF PRODUCT: SODIUM BENZOATE

SPECIFICATION

CHARACTERS   A WHITE, ALMOST ODOURLESS, CRYSTALLINE POWDER OR PRILL
IDENTIFICATION:

BENZOATES	POSITIVE
SODIUM	POSITIVE

APPEARANCE OF SOLUTION:

CLARITY	CLEAR
COLOUR	Y6
ACIDITY OR ALKALINITY (ml/g):	0.2MAX

HALOGENATED COMPOUNDS:

IONISED CHLORINE	200 ppm MAX
TOTAL CHLORINE	300 ppm MAX
HEAVY METALS(IN TERMS OF LEAD):	10 ppm MAX
ARSENIC:	3 ppm MAX
LEAD:	2 ppm MAX
MERCURY:	1 ppm MAX
READILY OXIDISABLE SUBSTANCES	POSITIVE
POLYCYCLIC ACIDS	POSITIVE
LOSS ON DRYING % (m/m):	1.5% MAX
ASSAY % (m/m):	99.0%-100.5%

ANALYZING METHOD   ACCORDING TO BP2013,EP8.0, E211, USP38, NF33, FCC9

APPENDIX C: Spec- Sodium Benzoate

Xanthan Gum

Specification

Trade Name : **Xanthan Gum Food grade Mesh 80**

Chemical Formula : **$(C_{35}H_{49}O_{29})_n$**

Parameter	Standard
Appearance	White-Like or Light Yellow Powder
Particle size (mesh)	100% through 60 mesh not less than 95% through 80 mesh
Viscosity (1% KCL cps)	>1200
Sheer Ratio	≥6.5
V1/V2	1.02 – 1.45
pH (1% solution)	6.0 – 8.0
Loss on Drying (%)	≤15
Ashes (%)	≤16
Pb (ppm)	≤2
Total Nitrogen (%)	≤1.5
Pyruvic Acid (%)	≥1.5
Total plate count (CFU/g)	≤2000
Moulds/ Yeast (CFU/g)	≤100
Coliform (MPN/g)	≤0.3
Salmonella	Absent
Ethanol (mg/kg)	≤500

APPENDIX D: Spec- Xanthan gum

PRODUCT SPECIFICATION

Colloid Solution WJ-C1068
(Carageenan Gum)

Benefits
- Completely soluble at 80-90°C
- Sparkling clear and transparent gel
- For instant application with boiled water

Specification

- Moisture	12% max
- Particle size	60 mesh 80% pass
- Color	white to light yellow
- Viscocity (2.5% sol.,70°C)	50-100 cP
- pH (1.5% sol.,25°C)	7.0-10.0

Bacteriological

- Total plate count	3,000/g max
- Mold and Yeast	100/g max
- Salmonella	Negative
- E. coli	Negative

Packing : 25 kg/ ctn

Storage : store in cool and dry place, keep closing

Dosage : 2.5 g in 100 g water to form clear gel

APPENDIX E: Spec- Carageenan gum

Evachem

Evacaely Enterprise

23G, Medan Bukit Indah, 68000, Ampang, Selangor

Sales Line : 011-3741 2689

Specification Sheet

Refined Glycerin 99%

Paramater	Method	Specification
Glycerol Content %wt	APAG-GL-008	99.0% min
Moisture, %	USP 38	5.0 max
Color	USP 38	10 max
Chloride, ppm	USP 38	10 max
Sulphate, ppm	USP 38	20max
Fatty Acid & Esters (ml/0.5N NaOH/50g Glycerine)	USP 38	1.0 max

APPENDIX F: Spec- Glycerin

Evachem

Evachem Sdn Bhd

23G, Medan Bukit Indah 2, Taman Bukit Indah, 68000, Ampang, Selangor

Contact : 011-3741 2689

Specification

Product Name : Sodium Alginate Food Grade

Packing : 25KGS/BAG

Test	Parameters
VISCOSITY	1000 - 1900 CPS
MOISTURE	14 - 15
PH VALUE	6 - 7
Ca CONTENT	0.20

APPENDIX G: Spec- Sodium Alginate

UNIVERSITI TEKNIKAL MALAYSIA MELAKA